Monitoring of Formaldehyde column densities over Islamabad, Pakistan using MAX-DOAS instrument.

By

Kashif Imran

(00000277085)

A thesis submitted in partial fulfillment of the requirements for the degree of

Master of Science

In

Environmental Sciences

Institute of Environmental Sciences and Engineering (IESE)

School of Civil and Environmental Engineering (SCEE)

National University of Sciences and Technology (NUST) Islamabad, Pakistan

(2021)

THESIS ACCEPTANCE CERTIFICATE

It is certified that the contents and forms of the thesis entitled **"Monitoring of Formaldehyde column densities over Islamabad, Pakistan using MAX-DOAS instrument"** submitted by **Kashif Imran**, Registration No. **00000277085** has been found satisfactory for the requirements of the degree of Master of Science in Environmental Science.

Supervisor: _____
Dr. Muhammad Fahim Khokhar
Professor
IESE, SCEE, NUST

Head of Department: _____
Dr. Muhammad Fahim Khokhar
IESE, SCEE, NUST

Dean/Principal: _____
SCEE, NUST

CERTIFICATE

It is certified that the contents and forms of the thesis entitled **"Monitoring of Formaldehyde column densities over Islamabad, Pakistan using MAX-DOAS instrument"** submitted by Mr. Kashif Imran has been found satisfactory for the requirements of the degree of Master of Science in Environmental Sciences.

Supervisor: _____

Dr. Muhammad Fahim Khokhar

Professor

IESE, SCEE, NUST

Member:

_____

Dr. Muhammad Arshad
Associate Professor
IESE-SCEE, NUST

Member:

_____

Dr. Zeeshan Ali Khan
Associate Professor
IESE-SCEE, NUST

This thesis is dedicated to my Parents & Siblings *for their endless care, support, encouragement, and patience.*

Contents

List of Figures

Acknowledgment

First and foremost, I would like to thank **ALLAH ALMIGHTY,** the most gracious, the most beneficent, for allowing me to complete my MS degree and giving me courage and patience throughout my study. This dissertation would not have been possible without the guidance and the help of several individuals who in one way or another contributed and extended their valuable assistance in planning, executing, and finally, presentation of this study.

I would like to express my sincere gratitude to my thesis supervisor **Dr. Muhammad Fahim Khokhar** (IESE-SCEE) for his continuous support throughout my study, for his patience, motivation, enthusiasm, and immense knowledge. His guidance helped me through my research and writing of this thesis. I could not have imagined having a better advisor and mentor for my MS thesis.

Many thanks to **Dr. Muhammad Arshad** and **Dr. Zeeshan Ali Khan** (IESE-SCEE) for their guidance and support.

Kashif Imran

Abstract

Formaldehyde is a common organic compound. It is commonly found in the atmosphere through both natural and anthropogenic processes. The study focuses on monitoring of Formaldehyde column densities over Islamabad, Pakistan. Mini MAX-DOAS (Multi-Axis Differential Optical Absorption Spectroscopy) instrument was used for the stationary monitoring of formaldehyde. Monitoring was performed at IESE, NUST from Sep 2015 to Sep 2020. MAX-DOAS is used for the observation of formaldehyde to observe its behavior on an hourly, daily, monthly, and seasonal basis. The data obtained through MAX-DOAS is then analyzed through Q-DOAS software. Then daily averages are obtained using EXCEL. The daily averages obtained are compared with TropOMI and OMI, which shows a correlation of 0.61 and 0.63 respectively. Temperature shows a direct correlation of 0.64 with formaldehyde column densities while global horizontal irradiance shows an inverse correlation of 0.09 with formaldehyde concentration. The Seasonal-based comparison shows the highest concentration during monsoon followed by Post Monsoon, Pre-Monsoon and winter respectively.

Formaldehyde column densities from 23rd March 2019 to 15th April 2019, when there was no lockdown were compared with 23rd March 2020 to 15th April 2020 (lockdown period) to know the impact of smart lockdown on atmospheric Formaldehyde VCDs. The result shows a 9% decrease in formaldehyde column densities during the lockdown period. This shows that the smart lockdown has a significant effect on formaldehyde column densities.

Chapter 1

1. Introduction

1.1 Background

Earth is the only planet where life is possible and has an atmosphere. It provides us with fresh air to breathe. It also acts as a filter by absorbing harmful radiation from the sun. Therefore, it is mandatory for various living organisms. It is important to study its compositions, reactions, and other processes taking place in this layer of atmosphere. Volatile organic compounds (VOCs) are major atmospheric species. They are released through both natural and anthropogenic activities. Naturally, it can't be controlled but we can control its emission through anthropogenic sources to avoid its negative impacts. The concentration of numerous VOCs is reliably higher inside (up to multiple times higher) than outside. Plants release various gases under stress due to environmental changes. The emission could incorporate different nonoxygenated and oxygenated natural mixtures, like green leaf volatiles (GLVs), terpenes, and sweet-smelling compounds. terpenes, including monoterpenes (C10), isoprene (C5), sesquiterpenes (C15), and homoterpenes (C11), are antecedents for aerosol formation. They also act as cloud condensation nuclei and influence the oxidization capacity of the atmosphere (Spracklen et al., 2011). Pollution in Pakistan is nowadays the major issue due to its detrimental effect on humans and the environment. During the last few decades, it causes severe damage to human health and the environment and is being ranked as the greatest environmental risk to human health (Anjum et al., 2021). Air pollution is a continuously growing problem due to its impact on health, ecosystems, and climate. According to the World Health Organization, more than 6.5 million people died annually because of air pollution (WHO 2016). Air can be polluted through both natural and anthropogenic sources. It can cause harm to all living organisms and their environment. With the increase in population, the need for food and other requirements also increases. To meet them, industrialization is increasing. Also, urbanization leads to increase transportation. One of the major problems in our country is the lack of air quality monitoring stations.

1.2 Formaldehyde

Formaldehyde is a ubiquitous trace gas that is harmful to the environment as it is present everywhere. Formaldehyde (HCHO) is a major hydrocarbon in our atmosphere. Mainly it is found in the troposphere. It is used to identify the emission of photochemical activity as well as non-methane volatile organic compounds (NMVOC). HCHO is primarily produced from fossil fuel combustion. Formaldehyde is found in the atmosphere and is attributed to the most abundant aldehyde in the atmosphere (Salthammer, 2013).

Formaldehyde can be emitted both naturally or by human activities. Naturally, it can be emitted by vegetation, forest fires. Its anthropogenic sources include fuel combustion, including mobile sources such as automobiles, and stationary sources such as Industries. It can get into the air by materials containing formaldehyde. It releases gases or vapors into the air. Automobile exhaust is the main source of formaldehyde. Appliances that use fuel such as wood-burning stoves, gas stoves, and kerosene heaters can also contribute to formaldehyde concentration.

1.3 The Present Study

The study is conducted to monitor the column amounts of formaldehyde and to compare it with satellite observations. Column densities of formaldehyde were measured using the Mini MAX-DOAS instrument which is installed at the rooftop of the IESE-NUST, Pakistan. The data is analyzed using Q-DOAS software, then its VCDs are prepared using Microsoft Excel. It is then validated with satellite data. In this study satellite data obtained from both TropOMI and OMI as the data available for TropOMI starts from Sep 2018 onward so for previous years OMI's data was used.

1.4 Study Area

Stationary monitoring of HCHO was carried at the IESE, NUST, Pakistan (Lat: 33.6479, Lon: 72.9896E).

1.5 Significance of Study

Air quality deterioration is one of the most concerning issues nowadays. The world's most polluted cities mainly include India, China, and Pakistan. The major cause of pollution in these countries is Automobiles, Industries, and agriculture burning (Khokhar et al., 2015). This study will enable us to know the severity of air pollution in Pakistan, it may also help to

develop a future pathway to control air pollution. Other than that, the study helps to identify the sources of formaldehyde and its impacts on humans and their environment. This study also contributes to identifying the impact of smart lockdown on Formaldehyde column densities. The COVID-19 lockdown during 2020 resulted in a considerable drop in VCDs of HCHO and NO_2 during the lockdown (Tanvir et al., 2021). The study is designed to identify natural and anthropogenic sources of formaldehyde. Pakistan lacks an air quality monitoring station for trace gases in the atmosphere (Khokhar et al., 2016). This data opens the door to conduct further research for the betterment of air quality in Pakistan.

1.6 Objectives of Study

- Ground monitoring of formaldehyde concentrations over Islamabad, Pakistan.
- Comparison formaldehyde concentration obtained with Max-DOAS measurements with results of satellite observations.

Additional: The effect of smart lockdown on Formaldehyde VCDs.

Chapter 2

2. Literature Review

Air is a mixture of gases, some of these gases are harmful to humans and Environment. The atmosphere is the envelope of gases and water vapor surrounding the planet earth. As we move upward the density of these gases decreases. 75 percent of the total gases of the atmosphere fall in the troposphere. Nitrogen covers 78 percent and oxygen cover 21 percent of the atmosphere. The remaining 1 percent containing CO_2, CH_4, Ar, Ne, He, H, and Kr. There are a variety of gases in the atmosphere but here we will focus on formaldehyde.

Gases like CO, N_2O, O_3, HCHO, and CH_4 are trace gases that represent around 10 percent of Climate. Besides gases, there is a varying amount of water vapor in the air. There are few water vapors in the air in the desert areas whereas in the tropical region the air may contain up to 4 percent water vapors. This means the amount of water vapors varies from place to place. Other than these gases aerosols are also present. Aerosol is comprised of particles of solid and drops of liquid. Aerosols can be natural aerosols such as fog, mist, dust, forest exudates, geyser system, biological materials, soil, sea salts, and minerals dust. Anthropogenic sources include (Incomplete combustion of fossil fuels, biomass burning, and industrials particulates. (Ramanathan et al., 2001)

2.1 Trace gases in the atmosphere

There is a large number of trace gases present in the atmosphere like N_2O, CH_4, HCHO, NOx, CO, SO_2, and O_3. An exponential increase in the combustion of fossil fuel, deforestation, automobiles, industrialization, and biomass burning increases the concentration of trace gases. Some trace gases are present in very low concentrations, they still have a significant effect in trapping the IR radiation contributing to global warming. Many trace gases strongly absorb IR radiation and perturbate the earth's radiation energy balance, contributing to the greenhouse effect and global warming. (Dickinson & Cicerone, 1986). HCHO is an active gas in the presence of sunlight it can generate HO_2 free radical by photolysis which in turn quickly reacts with NO to form hydroxyl radicals. These radicals impact the oxidation capacity of the atmosphere (Tian et al., 2018)

2.2 Volatile Organic Compounds

VOCs are hydrocarbons having high vapor pressure at room temperature. Vapor pressure is inversely proportional to B.P. VOCs are important atmospheric compounds and have a significant effect on Environment. It is harmful to both humans as well as Environment. The main sources are oceans, biomass burning, fossil fuel burning, and geochemical processes (Vrekoussis et al., 2010).VOCs are mainly synthetic compounds that release effectively in the atmosphere, they are found in solid and liquid forms. VOCs mainly contain numerous indoor items like paints, stains, cleaning items, beauty care products, pesticides, building materials, office hardware, cement, and so forth. VOCs are diverse chemicals that are volatile. VOCs also contain gasoline, combustion products of wood, and fuels; automobiles emission and smoke of tobacco are the most important source of BTEX in an outdoor and indoor environment (Anand et al., 2014). Non-methane volatile organic compounds ultimately convert into ozone and secondary organic aerosols (Nourian et al., 2021).

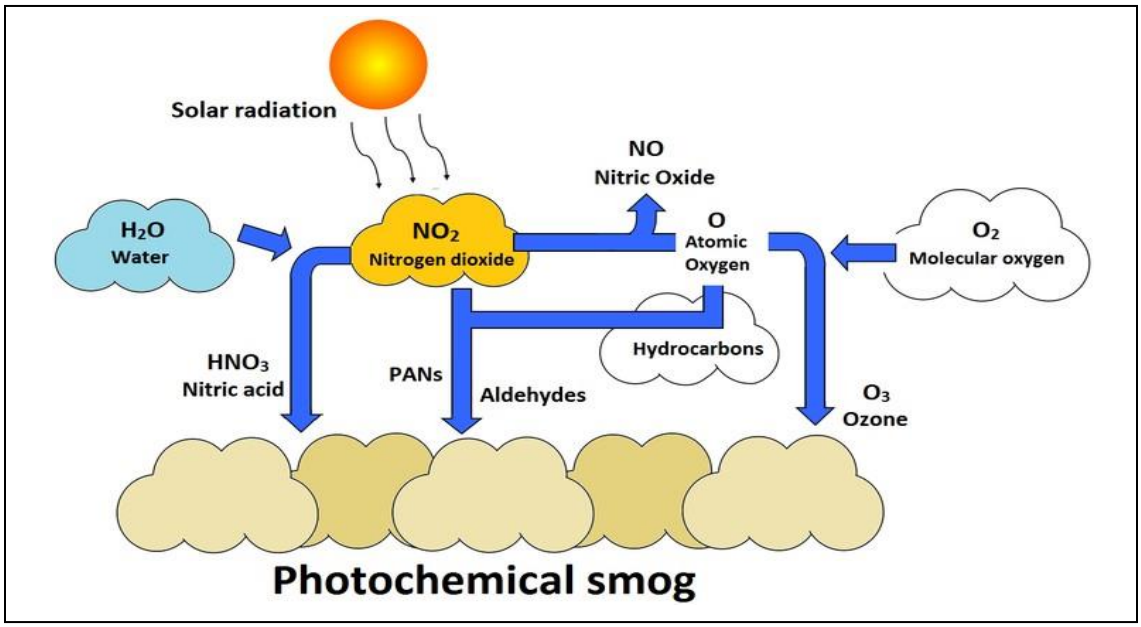

Figure 2.1: **Formation of photochemical smog**

Nonmethane volatile organic compounds are released both naturally and by anthropogenic sources. Nonmethane volatile organic compounds include xylene, benzene, propane, and butane. It mainly releases from Industrial processes, the use of organic solvents, and transportation. Most important NMVOCs are released from nonmethane hydrocarbons. One of the common NMVOCs is isoprene. It is being emitted from vegetation and absorbs

oxidants, acting as a sink for NO thus competing with ozone and can allow long-distant transport of nitrogen, contributing to nitrogen sequestration (Guenther et al., 2000). Anthropogenic sources of NMVOCs include vehicular emissions and refineries (Watson et al., 2001)

Methane is present everywhere. It is considered a stronger greenhouse gas as compared to CO_2 as its heat-trapping capacity is 21 times more than CO_2. Methane reacts with OH radicals to form ozone, formaldehyde, and CO in the presence of a high concentration of NOx.

2.3 Formaldehyde

Formaldehyde is a trace gas having no color, it is flammable but has a strong smell. It is used to make building materials and also to produce different medical preservatives and household products. In the atmosphere it is released by anthropogenic and biogenic sources but also produces by the reaction of methane and non-methane VOCs with oxygen which contributes up to 90 percent of total formaldehyde in the atmosphere (Pamler et al., 2003)

2.4 Atmospheric chemistry of HCHO

VOCs upon Photochemical degradation produce formaldehyde. Formaldehyde products depend upon the season, time, and location. Among VOCs methane is the major VOC that contributes to formaldehyde concentration. Formaldehyde can be produced in several ways. It can be formed by the reaction of hydroxyl with methane in the presence of oxygen. In case of a high concentration of NOx, methyl peroxyl get reacts with nitric oxide to produce methoxyl which further oxidizes to produce Formaldehyde (Luecken et al., 2012).

$$CH_4+OH+O_2 \rightarrow CH_3O_2 + H_2O$$

$$CH_3O_2+NO \rightarrow CH_3O+NO_2$$

$$CH_3O+O_2 \rightarrow HCHO+HO_2$$

Monoterpenes and isoprene are released from plants. They are a major emitter of Carbon. (Ryan et al.,2020). Methane absorbs OH in the ocean, monoterpenes, and isoprene readily reacts on land; hence, they play an important role in determining oxidative capacity (Porter et al., 2017) Photolysis and hydroxyl reactivity decrease the HCHO lifetime by up to 2 hours. Isoprene is among the important biogenic VOC, having a very short lifetime, and quickly

oxidizes into formaldehyde by undergoing various atmospheric reactions (Sprengnether et al., 2002).

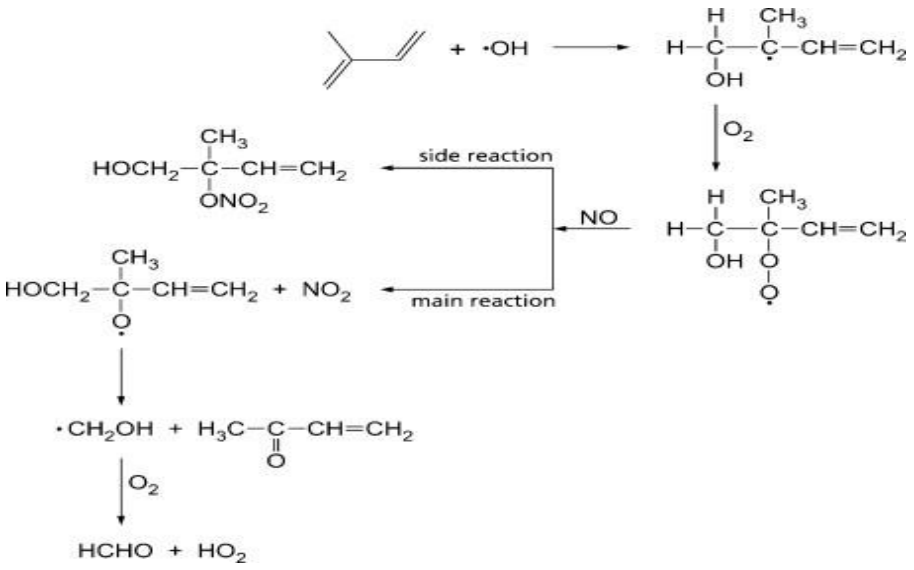

During the daytime, in the presence of sunlight, and reaction with hydroxyl radicals is the major sink of HCHO. The wet and dry deposition also removes HCHO from the atmosphere. Also, at nighttime HCHO is removed at slower rates from the atmosphere by reacting with nitrate radical (Wuebbles & Hayhoe, 2002).

2.5 Sources of Formaldehyde

The primary emission sources of formaldehyde in the atmosphere are fossil fuel combustion, forest fires, seawater, wood processing, plant, waste decay, and biofuel burning. The secondary sources of HCHO are photochemical oxidation of non-methane and methane VOCs in the atmosphere that is released by industries, biomass burning, fossil fuel combustion, animals, and vegetation (Chen et al., 2017).

2.6 Sink of Formaldehyde

There are three major pathways by which HCHO is take off from the atmosphere i.e., removal via photolysis, Hydroxyl oxidation, and wet and dry deposition. The removal via photolysis is carried out through two pathways,

$$HCHO + hv \rightarrow H_2 + CO$$

$$HCHO + hv \rightarrow H + HCO$$

While removal via OH oxidation takes place by reaction of OH radicals with HCHO (Cantrell et al.,1990),

$$HCHO + OH \rightarrow HCO + H_2O$$

$$HCO + O_2 \rightarrow HO_2 + CO$$

2.7 Health impacts of HCHO

The climate of Islamabad is a subtropical humid climate. Urbanization is a major driver of environmental change, and socioeconomic development shows little indication of abatement causing serious health impacts (Wang et al., 2020). Formaldehyde is an unfavorably susceptible (immunologically intervened) skin sensitizer that may likewise cause or worsen respiratory problems in people with previous or formaldehyde-instigated bronchial hyperreactivity. Formaldehyde gas is an exceptionally receptive alkylating specialist which is mutagenic in a few in vitro test frameworks. formaldehyde openness ought to be treated like it represents a cancer-causing hazard to people and ought to be decreased to the most reduced possible level. Humans are exposed to formaldehyde in both outdoor and indoor environments and food. HCHO exposure leads to many adverse human health effects. Many cases of HCHO exposure from contaminated food, polluted water, and air have been documented in the past two decades. Numerous such cases have raised public concern about the health effects of HCHO exposure as these exposures have affected human health negatively. Today the concern about HCHO health effects continues to grow worldwide due to the increased levels of exposure.

2.7.1 Acute effects

Irritation of the throat, nose, and eyes are the major effects of acute HCHO exposure. Human bodies come in contact with HCHO through ingestion, inhalation, and dermal exposure. Its acute exposure also causes chest pains, wheezing, coughing, and bronchitis. Other effects include ulcer formation in the mouth and stomach and also cause corrosion of the gastrointestinal tract (Kim et al., 2011).

2.7.2 Chronic Effects

In humans, Chronic HCHO exposure via inhalation is responsible for irritating the nose, throat, and eyes. When HCHO comes in contact with skin repeatedly in liquid form, it causes skin irritation and skin allergies (Tang et al., 2009). Considering the effects on the respiratory system of humans, a minimum concentration of 0.003 ppm has been assigned for HCHO long-term inhalation (Chou & Williams-Johnson, 1998). Inhalation of formaldehyde in high concentration can cause serious health impacts such as lung failure, stimulation of mucous membranes results from chronic exposure to HCHO. It is now categorized as a carcinogen for humans. ("The World Health Report 1996 - Fighting Disease, Fostering Development," 1997).

2.7.3 HCHO- A human carcinogen

HCHO has been ranked in Group B1 of chemicals by EPA and is considered a probable human cancer-causing agent (United States Protection Agency, 2001). However, it was placed in Group 1 by International Agency for Research on Cancer (IARC) and was classified as a human carcinogen later it was again assigned as a B1 carcinogen. According to IARC HCHO is a nasopharyngeal cancer-causing agent (IARC Working Group on the Evaluation of Carcinogenic Risks to Humans, 2012). Ingestion of formaldehyde can cause death, and long-term exposure to low levels in the atmosphere all around or on the skin can cause respiratory issues like asthma and skin diseases like dermatitis and tingling. Groupings of 100 ppm are promptly risky to life and well-being. A few people may have unfriendly impacts like consuming sensations in the eyes, nose, and throat; hacking; wheezing; queasiness; watery eyes; and skin aggravation.

2.7.4 Effect of COVID-19 smart lockdown on Formaldehyde column densities

COVID-19 has a significant effect on Formaldehyde concentration. Different studies indicate that lockdown has a significant effect on Formaldehyde concentration. Formaldehyde concentration decreases during the lockdown period. The average VCDs of NO_2 and HCHO as observed from the MAX-DOAS instrument were lower in 2020 as compared to the same days in 2019 (Tanvir et al., 2021). VCDs of NO_2, HCHO, and SO_2 for the study period. Phase-1 lockdown had a significant impact on the reduction of trace gases, especially NO_2, while HCHO and SO_2 depict a relatively lower-level reduction as compared to NO_2. (Javed et al., 2020).

2.8 DOAS Technique

MAX-DOAS is used for the measurement of trace gases in the atmosphere. MAX-DOAS instrument uses different elevation angles between 0 and 90° to measure stray light above the horizon. The MAX-DOAS instrument is designed in such a way to have a minimum error, very few even less than a percent, which allows detecting various trace gases (i.e., O_3, HCHO, CHOCHO, NO_2, and SO_2) in UV and visible spectral ranges even in the environment where the pollution level is low (Khan et al., 2018). The DOAS principle can be applied to various ground-based, ship-based, aircraft-based, and satellite-based platforms (Platt et al., 2008).

2.8.1 Working principle of DOAS

MAX-DOAS works on Lambert-Beer law. It states that absorption is directly proportional to concentration. $\mathbf{I(\lambda)=Io\ (\lambda)\ e^{-\alpha LC}}$

"I" as measured intensities

"Io" refers to the incident flux.

σ(λ): absorption cross-sections (cm_2 molecule−1)

L: pathlength (cm)

n: number density of the species (molecules/cm_3)

The presence of several gases, aerosols, and processes such as scattering processes (Rayleigh, Mie and, Raman) limits the application of the Lambert-Beer law. The DOAS technique is used to solve such problems partially or entirely. This technique depends on the difference in wavelength is observed and reference radiances. Different trace gases are determined by absorption capacities in the UV/visible cross-sections of suitable molecules which include HCHO, O_3, SO_2, and NO_2. In the beginning, it was developed for ground-based observation and has now been modified to measure different space-borne spectrometers as well (Platt et al., 2008).

2.8.2. DOAS instrumentation

Both active and passive instrumentation can be used in the DOAS technique. In both types of instrumentation, a light source is required. Passive DOAS requires extraterrestrial light sources such as sun, starlight, or moon.

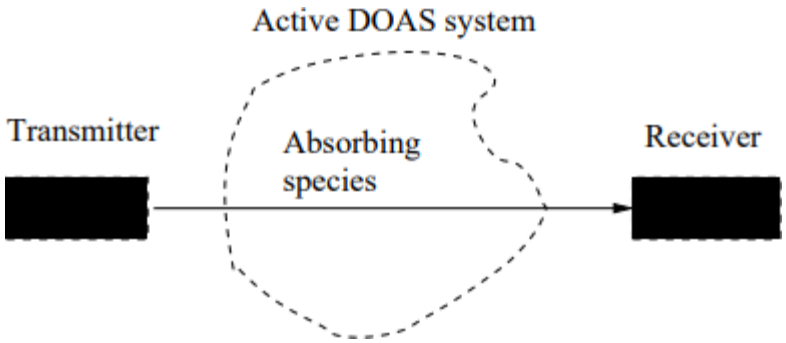

2.8.3 Advantages of DOAS Technique

MAX-DOAS measures several trace gases simultaneously, it saves time for measurement and enables the analysis of different chemical components in the air. The DOAS principle can be applied to various ground-based, ship-based, aircraft-based, and satellite-based platforms (Platt et al., 2008). Moreover, in the case of the DOAS technique, Mie and Rayleigh's scattering can be excluded. Due to its long path lengths, it is a highly sensitive technique (Hönninger et al., 2004).

2.8.4 Disadvantages of DOAS Technique

DOAS system doesn't work properly in rainy and snowy conditions. Also, a confined number of atmospheric species have appropriate abortions in the UV-visible region (Platt et al., 2008).

2.9 Tropospheric Ozone Monitoring Instrument

It works on the phenomenon to observe sunlight that is scattered back to space by Earth's surface and atmosphere, detecting the number of gases in the atmosphere by making a spectrum. TropOMI absorbs measures in the near-infrared (675–775 nm), ultraviolet and visible (270–500 nm), and shortwave infrared (2305–2385 nm) spectral bands. This means that a wide range of pollutants such as NO_2, O_3, HCHO, SO_2, CH_4, and CO can be imaged more accurately than ever before. It has a resolution as high as 7 km × 3.5 km, it has the potential to detect air pollution from a very small to large scale. The target is to contribute to monitor air quality and provide critical information. This helps decision-makers to take good steps. With its open data policy, and global coverage the mission will support global efforts to monitor pollution and improve our understanding of chemical and physical atmospheric processes.

Chapter 3

3. Materials and Methods

In this research, Mini-MAX-DOAS was used with the dimensions 13cm ×19cm ×14cm. It has fully automatic functions. It is specifically used for the measurement of scattered sunlight. A quartz lens that has a focal length of 40mm collects and focuses the light scattered by the sun in a spectrometer via optical cables. The spectrometer is installed in the instrument having a spectral resolution of 0.7nm from Ocean Optics Inc. and model no is USB2000+ crossed Czerny-Turner. It consists of a CCD-detector (one-dimensional) having a spectral range of 320-465nm and have 2048 pixels. To adjust the viewing direction of the instrument at desired elevation viewing angles with a precision of 0.1 degrees/step and 666Hz frequency, a stepper motor is used. The spectrometer was cooled by using Peltier cooling system to maintain a stable temperature. Windows 7 is used to control the functions of the instrument.

Figure 3. 1: ***Mini MAX- DOAS***

3.1 Monitoring sites and schedule

The Mini-MAX-DOAS was used for the fixed monitoring of HCHO. It was mounted on the rooftop of IESE, NUST-Islamabad for continuous fixed monitoring with elevation viewing angle settings of 2°, 4°, 5°, 10°, 15°, 30°, 45°, and 90°. The reason for choosing an angle of 90° was avoidance of interferences that might be caused by nearby substances while at the angle of 30° calculation of geometric Air Mass Factor (AMF) is easier.

3.2 Algorithms and tools

Formaldehyde was measured, analyzed, and plotted by using different software listed in table 3.2:

Table 3.2: List of Software used during the research work.

Sr. #	Software	Purpose
1	DOASIS (Differential Optical Absorption Spectroscopy Intelligent System) (v 3.2.35)	Operating Software for MAX-DOAS and measurement of back scatter intensities
2	WinDOAS (Windows Differential Optical Absorption Spectroscopy)	Calibration process is performed.
3	QDOAS (v. 2.111.1)	Analysis of UV-Visible spectra to retrieve DSCDs
4	Microsoft Excel (v. 2016)	Mathematical Calculations for tropospheric VCD extraction and Graphical representations
5	ArcGIS (v. 10.3.1)	Interpolation of OMI Data and Validation of MAX-DOAS data with satellite observations

3.3 DOAS intelligent system (DOASIS)

The mini-Max-DOAS was operated by DOASIS software to acquire data. The software is run by JavaScript with customized commands. The program adjusted the integration time of measured spectra, controlled the movement of the instrument by a stepper motor, and regulated the temperature of the spectrometer. The ring spectrum was also calculated by this software. Also, the software was used for zero correction of the MAX-DOAS instrument. For this purpose, the dark current and offset were measured both automatically and manually by

using DOASIS at night time. Offset is the measurement of spectra by the spectrometer in dark. It was measured by setting 1000 number of scans and an integration time of 100 milliseconds. Dark current on the other hand is the measure of a small electric current passing through the spectrometer. It was measured by selecting a number of scans to be 1 and the integration time of 10000 milliseconds.

3.4 HCHO Analysis

The analysis of HCHO was carried out by the following these three steps:

i Wavelength Calibration

ii Convolution of reference spectra

iii DOAS fit analysis of HCHO

The range selected for formaldehyde analysis was 336.5–359 nm. At this wavelength, we have the smallest possible residual (fit error). The spectrum which is best calibrated (fixed reference) measured at 90° is used as a reference spectrum for the analysis window. Elevation angles (2, 5, 10, 15, 30, 45 & 90°) are used for this study. The absorption cross-sections used were; HCHO at 298 K.

3.5 Wavelength Calibration

WinDOAS (Window differential optical absorption spectrometer) software was used for wavelength calibration. The spectrum at 90° with the highest concentration and the least solar zenith angle at noontime (11:30 – 12:30) was selected for the calibration of wavelength. The retrieved spectrum was fitted to the convoluted solar spectrum to perform the calibration of the instrument. Solar spectrum wavelength was allocated to a single detector's pixels for the fitting process. The calibration fit attained is also labeled as "Kurucz-fit". The range of wavelength was further split into 6 sub-windows for performance and analysis of fits in respective sub-windows. In the process of calibration, the shift of spectra amongst the measured and convoluted spectrum was adjusted by the function of "shift and squeeze". For the interpolation of the results of each sub-window, the Slit function indicating the polynomial

degree was utilized. By repeating the process of calibration several times, the residual error is minimized. The calibrated spectrum is used to calibrate the entire measured spectrums.

3.6 Convolution of reference spectra

An important mathematical method, convolution, is used in wavelength processing operations. For performing convolution QDOAS software was used and the option of "Convolution tool" was selected in the software. Convolution has two types: 1) Online convolution 2) Offline convolution. In online convolution preprocessing of cross-sections of various gases is not required because they get convoluted automatically during spectra analysis. In this type, cross-sections are simply put in formaldehyde analysis windows. While in the case of offline convolution, convolution of cross-sections is required before putting them in formaldehyde analysis windows. In this study, the online convolution method was used.

3.7 Convolution of cross-sections

The various cross-sections for trace gas used in the process of the convolution along with their specifications are enlisted in the table below.

Sr. #	Cross Section	Convolution
1	hcho_297K_Meller	Standard Convolution
2	o4_thalman_volkamer_293K_inAir	Interpolate
3	bro_223K_Fleischmann	Standard Convolution
4	no2_298K_vanDaele	Convolve Io (1e17 molecule/cm^2)
5	o3_223K_SDY_air	Convolve Io (1e20 molecule/cm^2)
6	o3a_243p223K_SDY_336-359nm	Convolve Io (1e20 molecule/cm^2)
7	Ring (Ring_QDOAScalc_HighResSAO_Norm)	Ring Convolution

Table 3.3: ***Details of cross-sections used with convolution specifications***

Gaussian shape was used as the slit function type with an FWHM of 0.7 nm. High-resolution cross-sections were convoluted by using the 'Standard convolution' option while for optical depth evaluation in the convolution, the 'Convolve I_0' option was selected (Fayt et al., 2013).

3.8 Analysis of HCHO

QDOAS software was used for analysis purposes. In the display tab, different fields (date, time, solar zenith angle, and elevation viewing angle) are selected as shown in the figure.

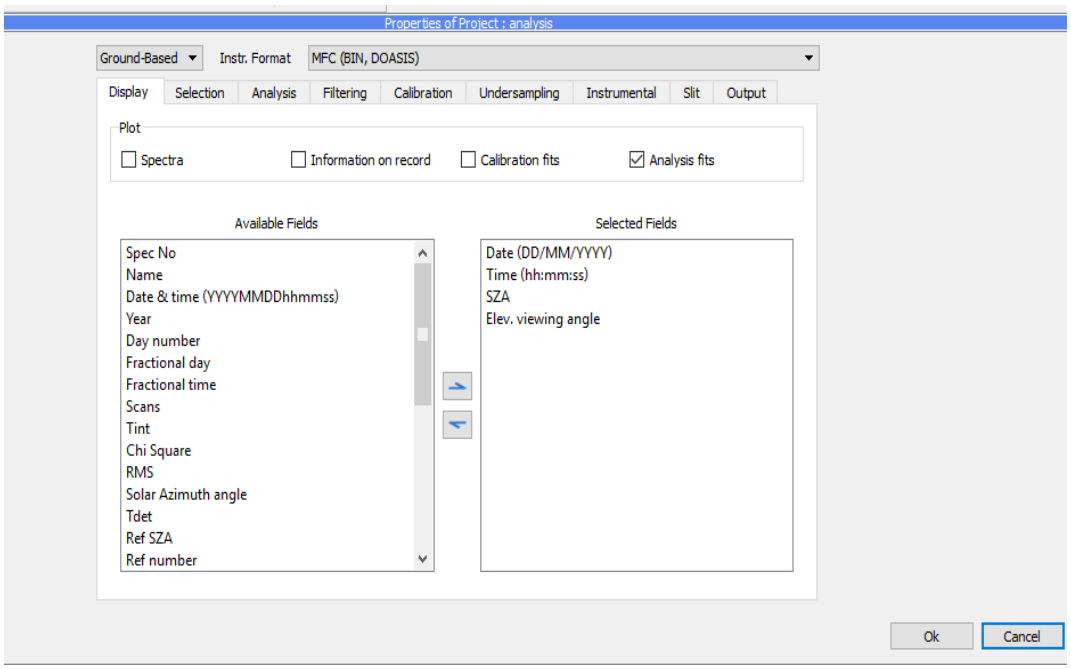

Figure 3.2: **Display tab on QDOAS software**

Then in the instrumental tab offset, dark current and calibration file is selected, and also the detector size of the instrument i.e., 2048 is entered manually.

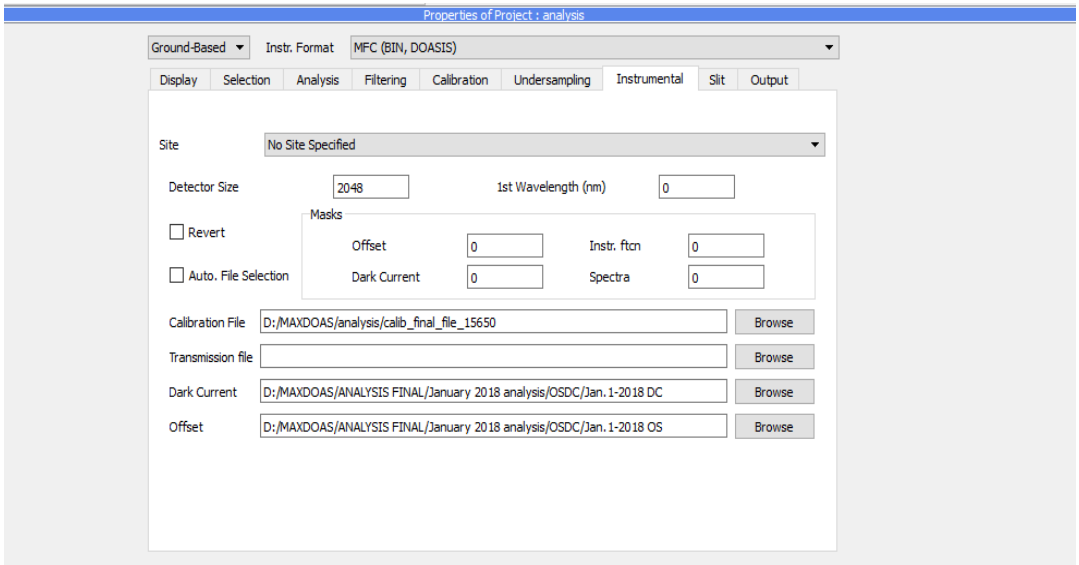

Figure 3.3: **Instrumental tab on QDOAS software**

In the properties of the analysis window for HCHO in QDOAS software, cross-sections along with their suitable convolution settings were added in the molecules tab. And the

fitting interval was set as 336.5-359nm. Also, the polynomial degree of order 5 was selected.

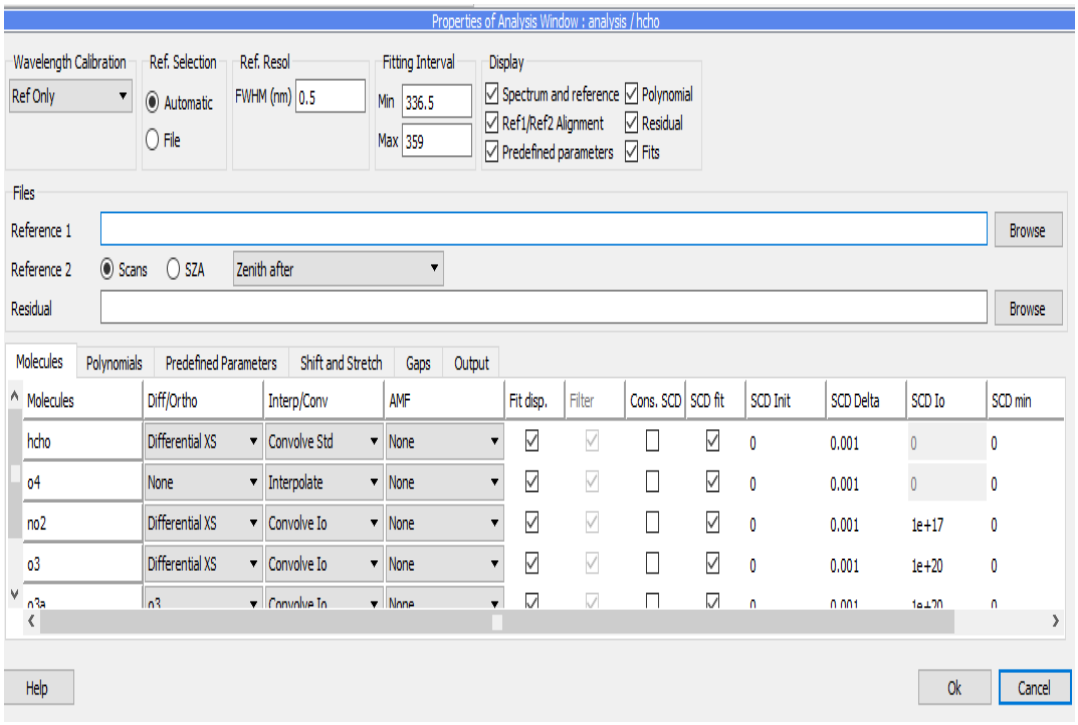

Figure 3.4: **Analysis window in QDOAS software**

Then the output path was selected and finally, analysis was run to obtain HCHO DSCDs in ASCII file format. These files containing the results of the analysis are opened by using Microsoft Excel.

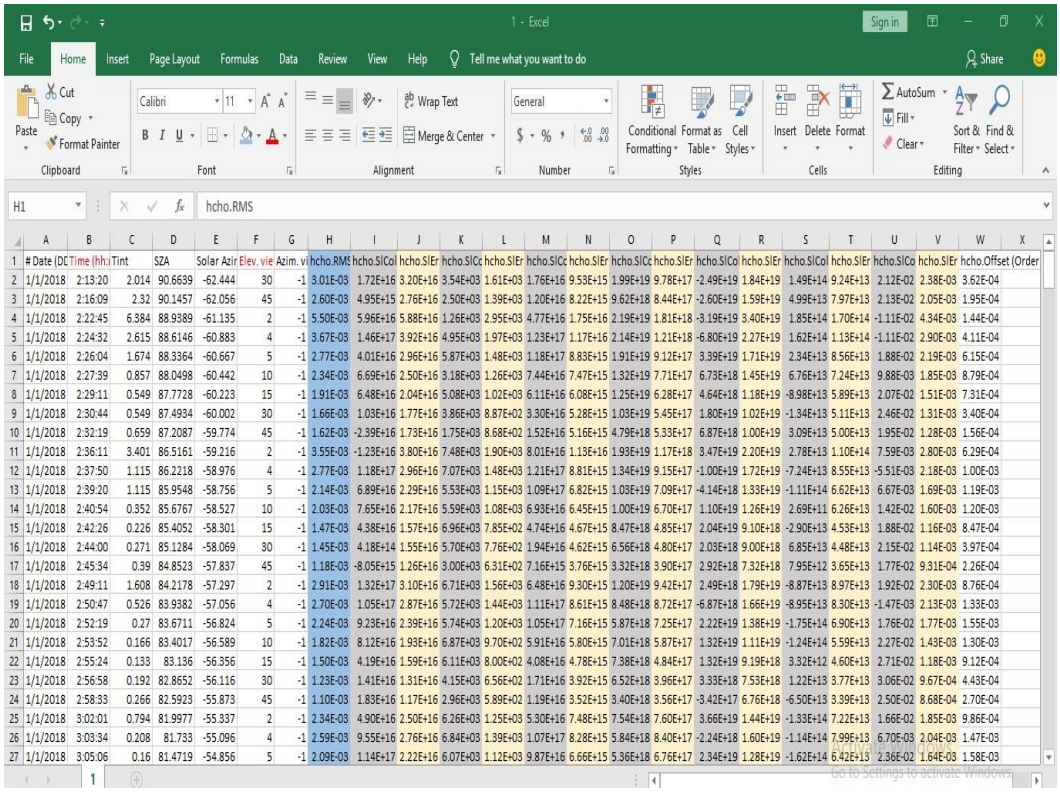

	A	B	C	D	E	F	G	H	I	J	K	L	M	N	O	P	Q	R	S	T	U	V	W	X
1	# Date (DC	Time (hh:r	Tint	SZA	Solar Azir	Elev. vie	Azim. vi	hcho.RMS	hcho.SlCol	hcho.SlEr	hcho.SlCc	hcho.SlEr	hcho.SlCc	hcho.SlEr	hcho.SlCc	hcho.SlEr	hcho.SlCo	hcho.SlEr	hcho.SlCo	hcho.SlEr	hcho.SlCo	hcho.SlEr	hcho.Offset (Order	
2	1/1/2018	2:13:20	2.014	90.6639	-62.444	30	-1	3.01E-03	1.72E+16	3.20E+16	3.54E+03	1.61E+03	1.76E+16	9.53E+15	1.99E+19	9.78E+17	-2.49E+19	1.84E+19	1.49E+14	9.24E+13	2.12E-02	2.38E-03	3.62E-04	
3	1/1/2018	2:16:09	2.32	90.1457	-62.056	45	-1	2.60E-03	4.95E+15	2.76E+16	2.50E+03	1.39E+03	1.20E+16	8.22E+15	9.62E+18	8.44E+17	-2.60E+19	1.59E+19	4.99E+13	7.97E+13	2.13E-02	2.05E-03	1.95E-04	
4	1/1/2018	2:22:45	6.384	88.9389	-61.135	2	-1	5.50E-03	5.96E+16	5.88E+16	1.26E+03	2.95E+03	4.77E+16	1.75E+16	2.19E+19	1.81E+18	-3.19E+19	3.40E+19	1.85E+14	1.70E+14	-1.11E-02	4.34E-03	1.44E-04	
5	1/1/2018	2:24:32	2.615	88.6146	-60.883	4	-1	3.67E-03	1.46E+17	3.92E+16	4.95E+03	1.97E+03	1.23E+17	1.17E+16	2.14E+19	1.21E+18	-6.80E+19	2.27E+19	1.62E+14	1.13E+14	-1.11E-02	2.90E-03	4.11E-04	
6	1/1/2018	2:26:04	1.674	88.3364	-60.667	5	-1	2.77E-03	4.01E+16	2.96E+16	5.87E+03	1.48E+03	1.18E+17	8.83E+15	1.91E+19	9.12E+17	3.39E+19	1.71E+19	2.34E+13	8.56E+13	1.88E-02	2.19E-03	6.15E-04	
7	1/1/2018	2:27:39	0.857	88.0498	-60.442	10	-1	2.34E-03	6.69E+16	2.50E+16	3.18E+03	1.26E+03	7.44E+16	7.47E+15	1.32E+19	7.71E+17	6.73E+18	1.45E+19	6.76E+13	7.24E+13	9.88E-03	1.85E-03	8.79E-04	
8	1/1/2018	2:29:11	0.549	87.7728	-60.223	15	-1	1.91E-03	6.48E+16	2.04E+16	5.08E+03	1.02E+03	6.11E+16	6.08E+15	1.25E+19	6.28E+17	4.64E+18	1.18E+19	-8.98E+13	5.89E+13	2.07E-02	1.51E-03	7.31E-04	
9	1/1/2018	2:30:44	0.549	87.4934	-60.002	30	-1	1.66E-03	1.03E+16	1.77E+16	3.86E+03	8.87E+02	3.30E+16	5.28E+15	1.03E+19	5.45E+17	1.80E+19	1.02E+19	-1.34E+13	5.11E+13	2.46E-02	1.31E-03	3.40E-04	
10	1/1/2018	2:32:19	0.659	87.2087	-59.774	45	-1	1.62E-03	-2.39E+16	1.73E+16	1.75E+03	8.68E+02	1.52E+16	5.16E+15	4.79E+18	5.33E+17	6.87E+18	1.00E+19	3.09E+13	5.00E+13	1.95E-02	1.28E-03	1.56E-04	
11	1/1/2018	2:36:11	3.401	86.5161	-59.216	2	-1	3.55E-03	-1.23E+16	3.80E+16	7.48E+03	1.90E+03	8.01E+16	1.13E+16	1.93E+19	1.17E+18	3.47E+19	2.20E+19	2.78E+13	1.10E+14	7.59E-03	2.80E-03	6.29E-04	
12	1/1/2018	2:37:50	1.115	86.2218	-58.976	4	-1	2.77E-03	1.18E+17	2.96E+16	7.07E+03	1.48E+03	1.21E+17	8.81E+15	1.34E+19	9.15E+17	-1.00E+19	1.72E+19	-7.24E+13	8.55E+13	-5.51E-03	2.18E-03	1.00E-03	
13	1/1/2018	2:39:20	1.115	85.9548	-58.756	5	-1	2.14E-03	6.89E+16	2.29E+16	5.53E+03	1.15E+03	1.09E+17	6.82E+15	1.03E+19	7.09E+17	-4.14E+18	1.33E+19	-1.11E+14	6.62E+13	6.67E-03	1.69E-03	1.19E-03	
14	1/1/2018	2:40:54	0.352	85.6767	-58.527	10	-1	2.03E-03	7.65E+16	2.17E+16	5.59E+03	1.08E+03	6.93E+16	6.45E+15	1.00E+19	6.70E+17	1.10E+19	1.26E+19	2.69E+11	6.26E+13	1.42E-02	1.60E-03	1.20E-03	
15	1/1/2018	2:42:26	0.226	85.4052	-58.301	15	-1	1.47E-03	4.38E+16	1.57E+16	6.96E+03	7.85E+02	4.74E+16	4.67E+15	8.47E+18	4.85E+17	2.04E+19	9.10E+18	-2.90E+13	4.53E+13	1.88E-02	1.16E-03	8.47E-04	
16	1/1/2018	2:44:00	0.271	85.1284	-58.069	30	-1	1.45E-03	4.18E+14	1.55E+16	5.70E+03	7.76E+02	1.94E+16	4.62E+15	6.56E+18	4.80E+17	2.03E+18	9.00E+18	6.85E+13	4.48E+13	2.15E-02	1.14E-03	3.97E-04	
17	1/1/2018	2:45:34	0.39	84.8523	-57.837	45	-1	1.18E-03	-8.05E+15	1.26E+16	3.00E+03	6.31E+02	7.16E+15	3.76E+15	3.32E+18	3.90E+17	2.92E+18	7.32E+18	7.95E+12	3.65E+13	1.77E-02	9.31E-04	2.26E-04	
18	1/1/2018	2:49:11	1.608	84.2178	-57.297	2	-1	2.91E-03	1.32E+17	3.10E+16	6.71E+03	1.56E+03	6.48E+16	9.30E+15	1.20E+19	9.42E+17	2.49E+18	1.79E+19	-8.87E+13	8.97E+13	1.92E-02	2.30E-03	8.76E-04	
19	1/1/2018	2:50:47	0.526	83.9382	-57.056	4	-1	2.70E-03	1.05E+17	2.87E+16	5.72E+03	1.44E+03	1.11E+17	8.61E+15	8.48E+18	8.72E+17	-6.87E+18	1.66E+19	-8.95E+13	8.30E+13	-1.47E-03	2.13E-03	1.33E-03	
20	1/1/2018	2:52:19	0.27	83.6711	-56.824	5	-1	2.24E-03	9.23E+16	2.39E+16	5.74E+03	1.20E+03	1.05E+17	7.16E+15	5.87E+18	7.25E+17	2.22E+19	1.38E+19	-1.75E+14	6.90E+13	1.76E-02	1.77E-03	1.55E-03	
21	1/1/2018	2:53:52	0.166	83.4017	-56.589	10	-1	1.82E-03	8.12E+16	1.93E+16	6.87E+03	9.70E+02	5.91E+16	5.80E+15	7.01E+18	5.87E+17	1.32E+19	1.11E+19	-1.24E+14	5.59E+13	2.27E-02	1.43E-03	1.30E-03	
22	1/1/2018	2:55:24	0.133	83.136	-56.356	15	-1	1.50E-03	4.19E+16	1.59E+16	6.11E+03	8.00E+02	4.08E+16	4.78E+15	7.38E+18	4.84E+17	1.32E+19	9.19E+18	3.32E+12	4.60E+13	2.71E-02	1.18E-03	9.12E-04	
23	1/1/2018	2:56:58	0.192	82.8652	-56.116	30	-1	1.23E-03	1.41E+16	1.31E+16	4.15E+03	6.56E+02	1.71E+16	3.92E+15	6.52E+18	3.96E+17	3.33E+18	7.53E+18	1.22E+13	3.77E+13	3.06E-02	9.67E-04	4.43E-04	
24	1/1/2018	2:58:33	0.266	82.5923	-55.873	45	-1	1.10E-03	1.83E+16	1.17E+16	2.96E+03	5.89E+02	1.19E+16	3.52E+15	3.40E+18	3.56E+17	-3.42E+17	6.76E+18	-6.50E+13	3.39E+13	2.50E-02	8.68E-04	2.70E-04	
25	1/1/2018	3:02:01	0.794	81.9977	-55.337	2	-1	2.34E-03	4.90E+16	2.50E+16	6.26E+03	1.25E+03	5.30E+16	7.48E+15	7.54E+18	7.60E+17	3.66E+19	1.44E+19	-1.33E+14	7.22E+13	1.66E-02	1.85E-03	9.86E-04	
26	1/1/2018	3:03:34	0.208	81.733	-55.096	4	-1	2.59E-03	9.55E+16	2.76E+16	6.84E+03	1.39E+03	1.07E+17	8.28E+15	5.84E+18	8.40E+17	-2.24E+18	1.60E+19	-1.14E+14	7.99E+13	6.70E-03	2.04E-03	1.47E-03	
27	1/1/2018	3:05:06	0.16	81.4719	-54.856	5	-1	2.09E-03	1.14E+17	2.22E+16	6.07E+03	1.12E+03	9.87E+16	6.66E+15	5.36E+18	6.76E+17	2.34E+19	1.28E+19	-1.62E+14	6.42E+13	2.36E-02	1.64E-03	1.58E-03	

Figure 3.5: **Microsoft excel sheet showing results of HCHO analysis performed in QDOAS software**

3.8.1 dAMF Calculation

Air mass factor was calculated by using Microsoft Excel. The ratio of direct incoming solar radiation path length to solar radiation path length coming vertically from the atmosphere is termed as the air mass factor (AMF). While Differential AMF is the AMF difference between $\alpha \neq 90°$ and $\alpha = 90°$ while $\propto$ being the elevation angle. The zenith view AMF can be evaluated as 1 (sin 90°-1), and the off-axis view AMF can be evaluated as 1/sinα respectively if the last scattering event of photons being recorded by the instrument happens to be higher than the layer of gas (Li et al., 2013).

dAMF(α) = 1/sinα – 1 **Eq.9**

3.8.2 Tropospheric VCD Calculation

The vertical column density (VCD) was calculated by converting AMF into dSCD. and from differential SCD, VCD was derived.

VCDgeo = dSCD (α) / dAMF(α) Eq. 10 VCDgeo = dSCD (α) / (1 / Sinα)1 Eq. 11

where α stands for elevation angle of the instrument, this specific method of calculating VCD is known as "geometric approach", therefore the VCD calculated are termed as VCDgeo.

3.8.3 Projection of Field Campaign VCDs

Maps were generated to present ground-based data monitored during the field campaigns along with satellite data for the respective days of the campaigns. ArcMap 10.3.1 was used to map the satellite data and ground based VCDs (as per the latitude and longitude measured using GPS).

3.8.4 Comparison of Ground-based results with satellite data

- The ground-based results were validated by comparing them with satellite data retrieved from OMI. Monthly Level 3 tropospheric satellite data was taken from the GIOVANNI website.

https://giovanni.gsfc.nasa.gov/giovanni/

- Also, satellite data from the Google earth engine was downloaded**.**

https://earthengine.google.com/

Chapter 4

4. Results and Discussion

4.1 HCHO Timeseries

Graph showing HCHO timeseries from Sep 2015 to Sep 2020. Trendline shows overall decrease in HCHO column densities from 2015-2020. This can be justified by a decrease in temperature during the time period. As temperature is the main source of HCHO release, during the study period temperature shows a relatively decreasing trend so is the HCHO column densities.

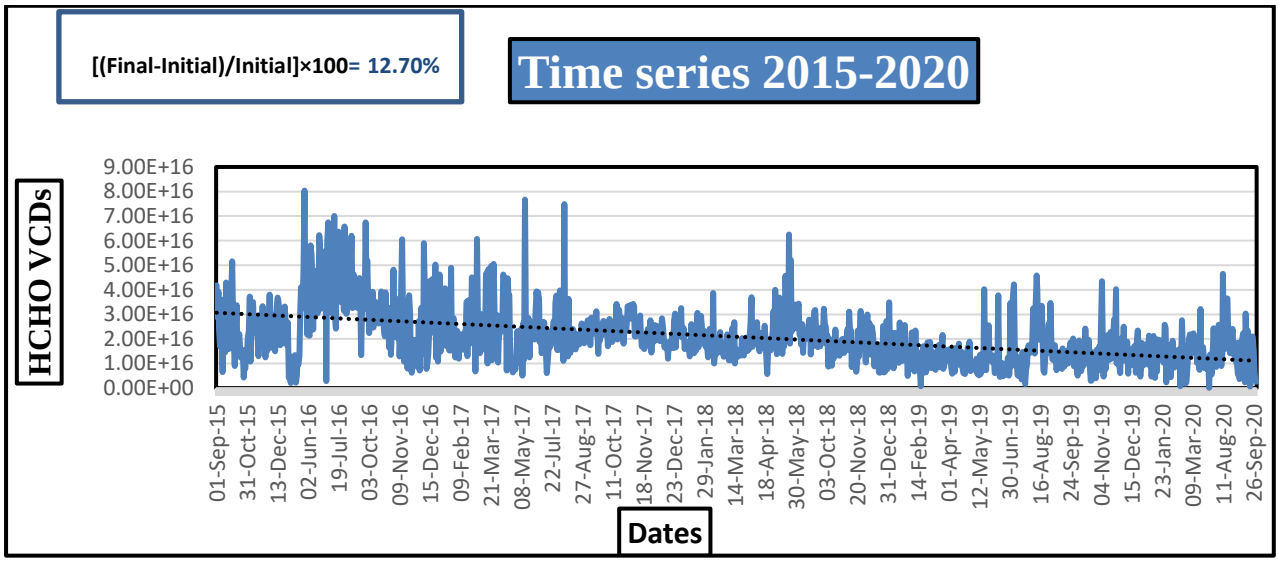

Figure 4. 1: Timeseries OF HCHO column densities from Sep 2015- Sep 2020.

4.2 HCHO diurnal cycle over IESE-NUST

From October 2018 to October 2020 hourly average of the calculated VCDs over IESE, NUST was taken. These averages were used to derive the diurnal cycle of the HCHO presented. In this graph, the annual HCHO diurnal cycle for 12 hours i.e., from 6 a.m. to 6 p.m. is shown because of the instrument's limitation as it only operates in the presence of sunlight.

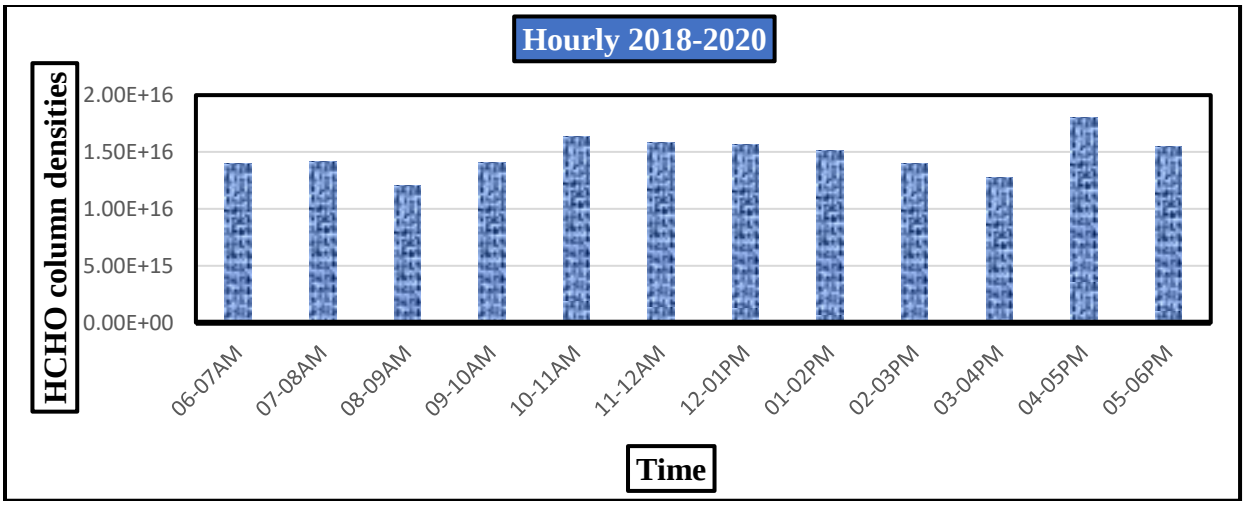

Figure 4. 2: Diurnal cycle (6 am- 6 pm) of average HCHO vertical column densities over IESE-NUST, Islamabad (Oct 2018-Oct 2020).

HCHO concentration was found maximum during the early hours and at evening time. It is higher in the morning because of the background concentrations and lower solar intensity. As the solar intensity starts increasing the HCHO concentration starts to decline reaching minima at 9 am due to photolysis and other chemical reactions. Till this time photolysis dominates over oxidation of methane and NMVOCs. However, from noontime and onward the HCHO concentrations start increasing as the temperature increase which increases the biogenic emissions and thus the increase in the rate of VOC oxidation as well.

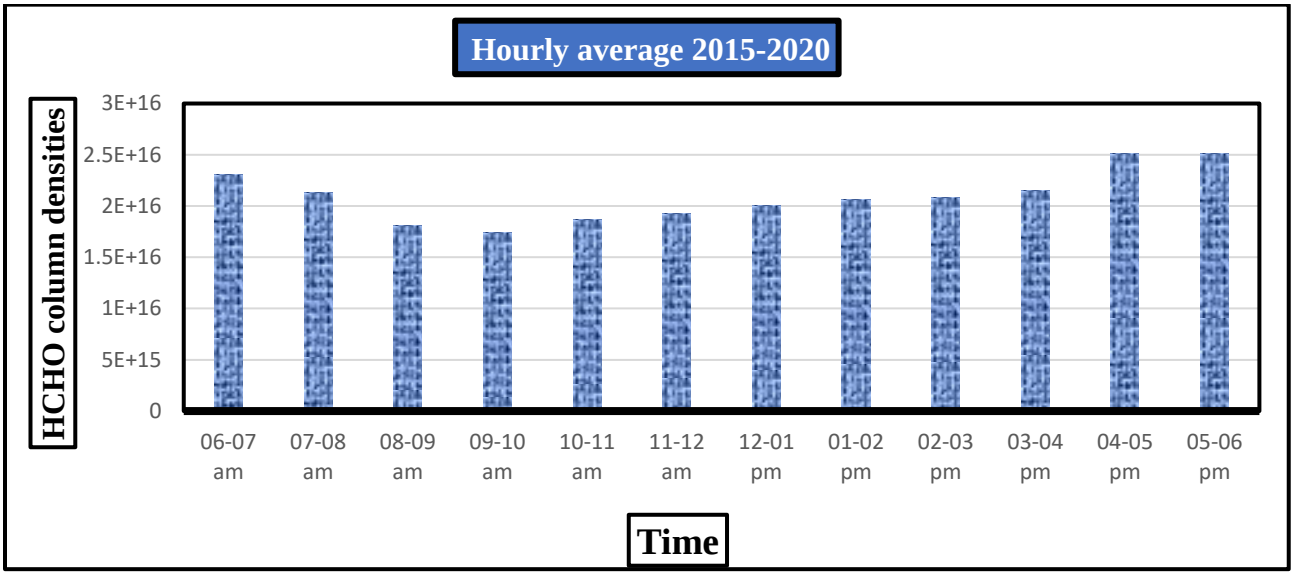

Figure 4. 3: Diurnal cycle (6 am- 6 pm) of average HCHO vertical column densities over IESE-NUST, Islamabad (Sept 2015-Oct 2020).

From 2015 to 2020 the chart shows an almost similar trend as in 2018-2020.

4.3 Seasonal Behavior

It can be observed that HCHO concentrations are found to be highest in Monsoon and lowest in the winter (Gratsea et al., 2016). which is mainly due to the increased amount of biogenic emissions of NMVOCs (HCHO precursors) such as isoprene in summer as they are released into the atmosphere as a response of plants to heat stress (Fini et al., 2017). While in winters plants are under minimum heat stress hence biogenic emissions are minimum. Also, HCHO values are higher during the early hours of winter. The reason for this could be the increased use of natural gas in offices and homes in the morning hours to cope up with cold weather, resulting in the increased level of methane in the atmosphere which upon oxidation forms HCHO as a byproduct. Moreover, in winters, solar intensity is lower which results in slower photolysis and results in higher background HCHO concentrations are present in the atmosphere.

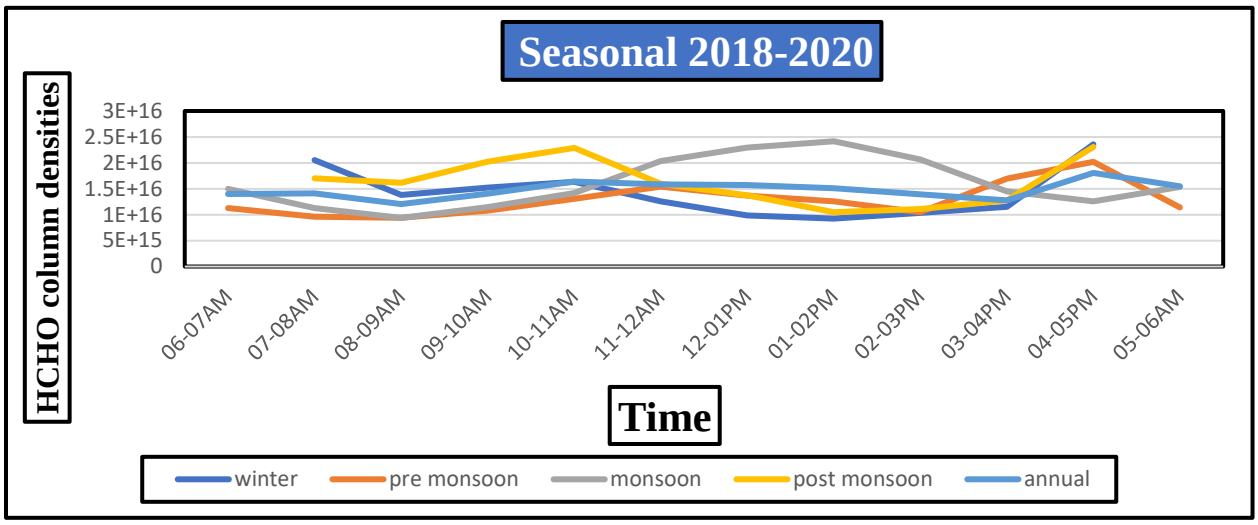

Figure 4. 4: Seasonal diurnal cycle (6 am- 6 pm) of average HCHO vertical column densities over IESE-NUST, Islamabad (2018-2020)

2015-2020 shows an almost similar seasonal trend. Highest in Monsoon, followed by Post Monsoon, Pre-Monsoon, and Winter.

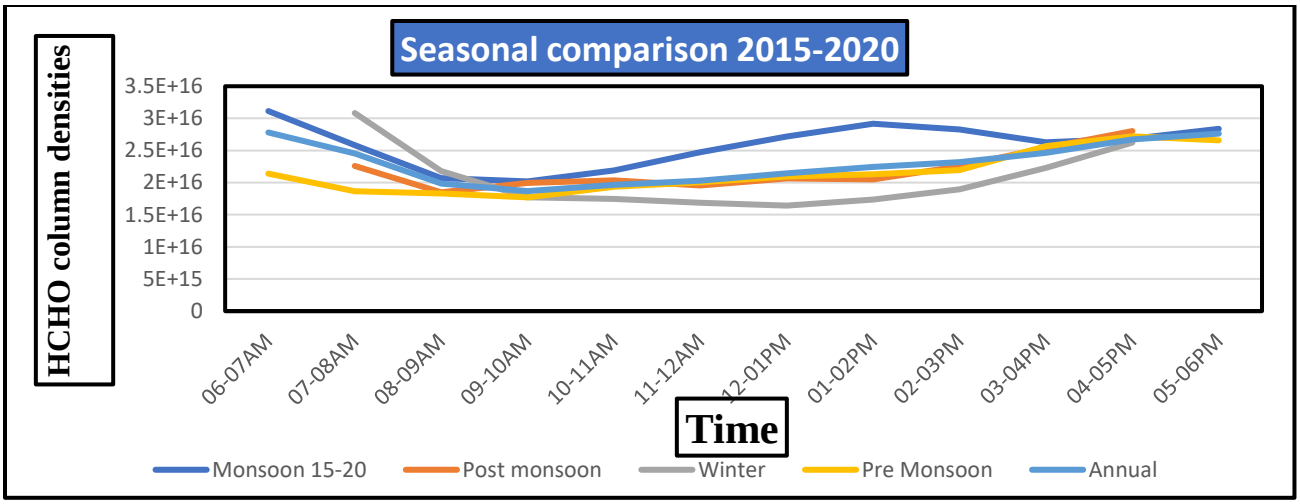

Figure 4. 5: Seasonal diurnal cycle (6 am- 6 pm) of average HCHO vertical column densities over IESE-NUST, Islamabad (Sept 2015-Oct 2020)

4.4 Weekly cycle of HCHO

The average weekly cycle shows the lowest concentration on Wednesday. This is due to the closure of the CNG station on Tuesday and Wednesday during the study period. Other than that Saturday and Sunday shows comparatively lesser concentration due to the weekend effect.

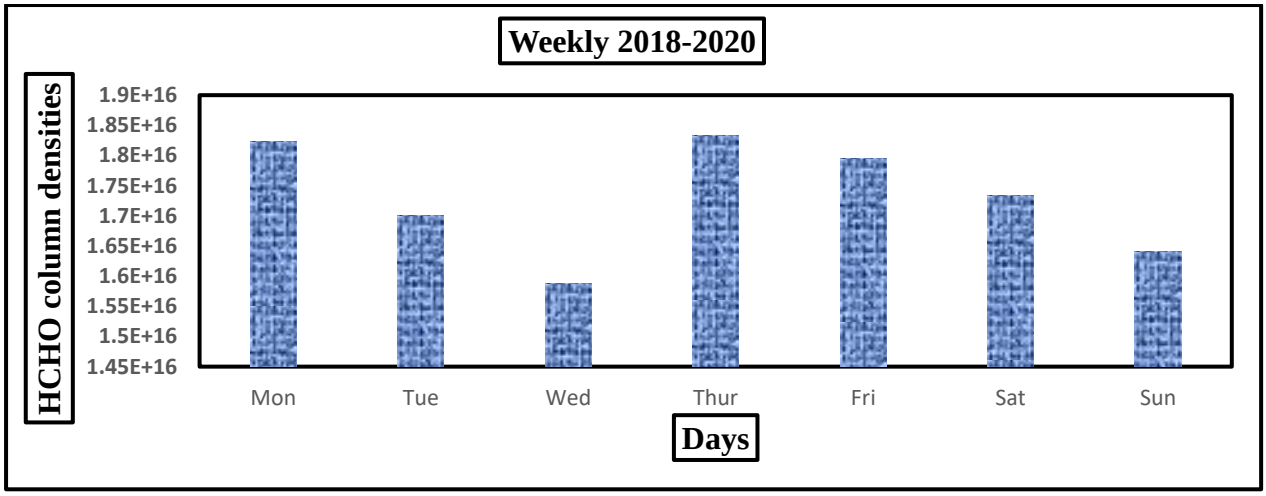

Figure 4. 6: HCHO weekly cycle over IESE-NUST monitored by using MAX-DOAS (Oct 2018-Oct 2020)

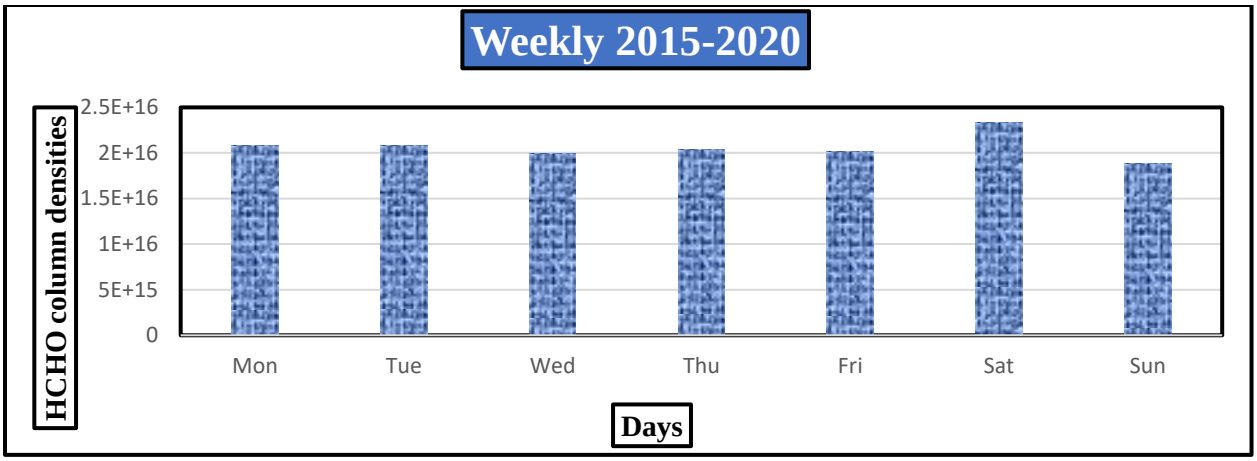

Figure 4. 7: HCHO weekly cycle over IESE-NUST monitored by using MAX-DOAS (Sept 2015-Oct 2020)

On the other hand, the weekly graph from 2015-2020 shows an almost similar trend throughout the week.

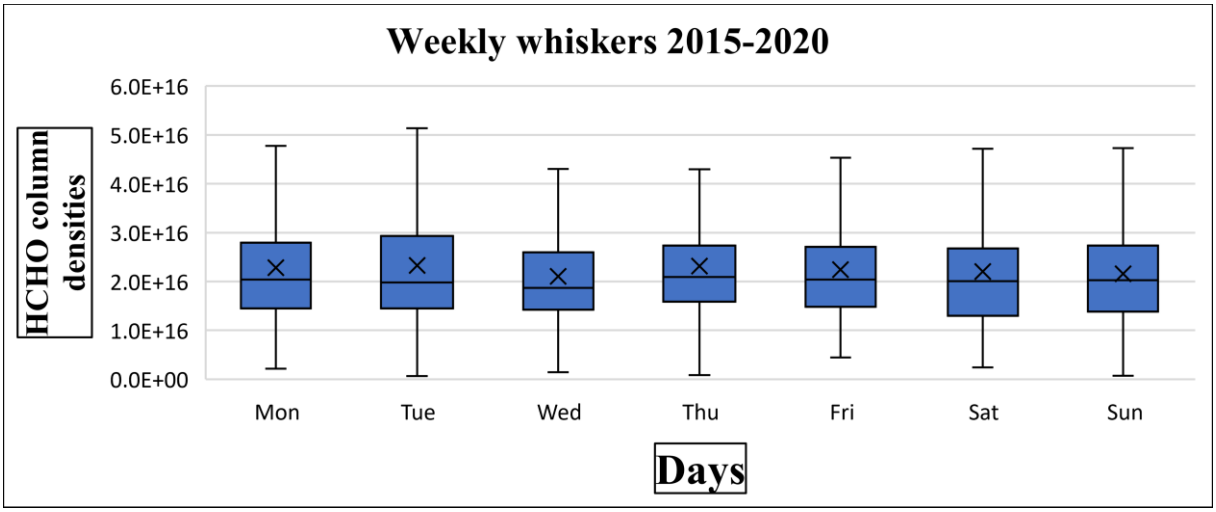

Figure 4. 8: weekly whiskers over IESE-NUST monitored by using MAX-DOAS (Sept 2015-Sep 2020)

These weekly whisker shows an almost similar trend throughout the week.

4.5 Monthly Comparison

The average monthly cycle of formaldehyde concentration from 2018-2020 was observed. The result shows the maximum concentration in June, July, and August. This is because of the summer effect. As in summer, the temperature is higher, so is the formaldehyde concentration.

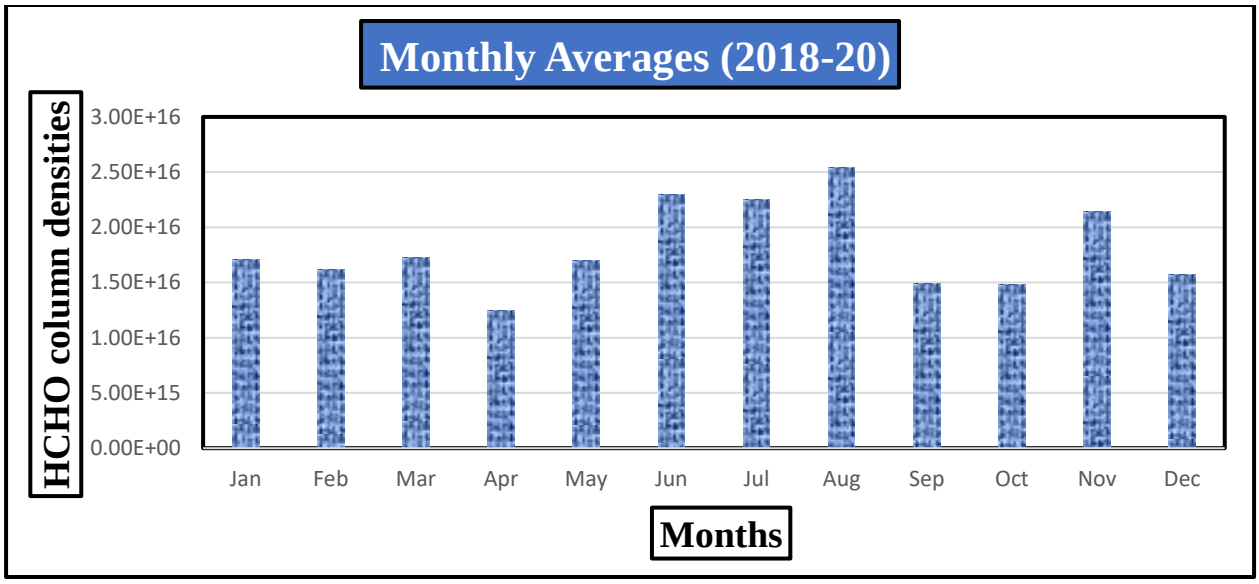

Figure 4. 9: HCHO monthly average VCDs over IESE-NUST observed using MAX-DOAS (Oct 2018-Oct 2020)

The graph shows the monthly trend from Sep 2015- Oct 2020, it is clear from the graph that in summer HCHO concentration is maximum while in winter it is minimum. The reason is the same as discussed above.

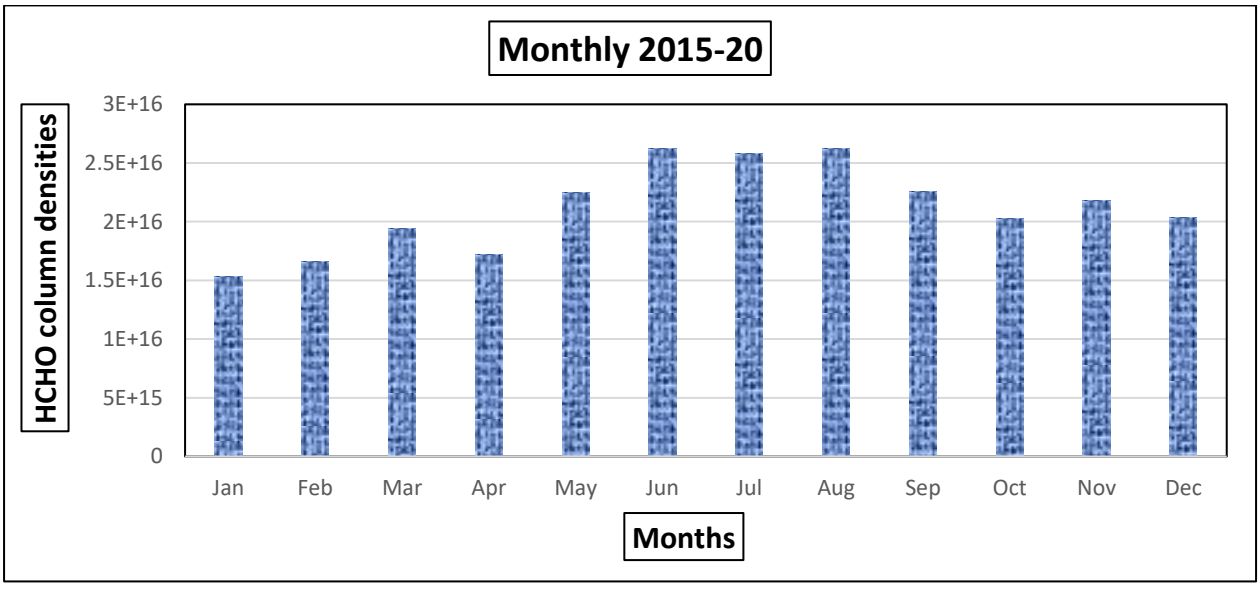

Figure 4. 10: HCHO monthly average VCDs over IESE-NUST observed using MAX-DOAS (Sep 2015-Oct 2020).

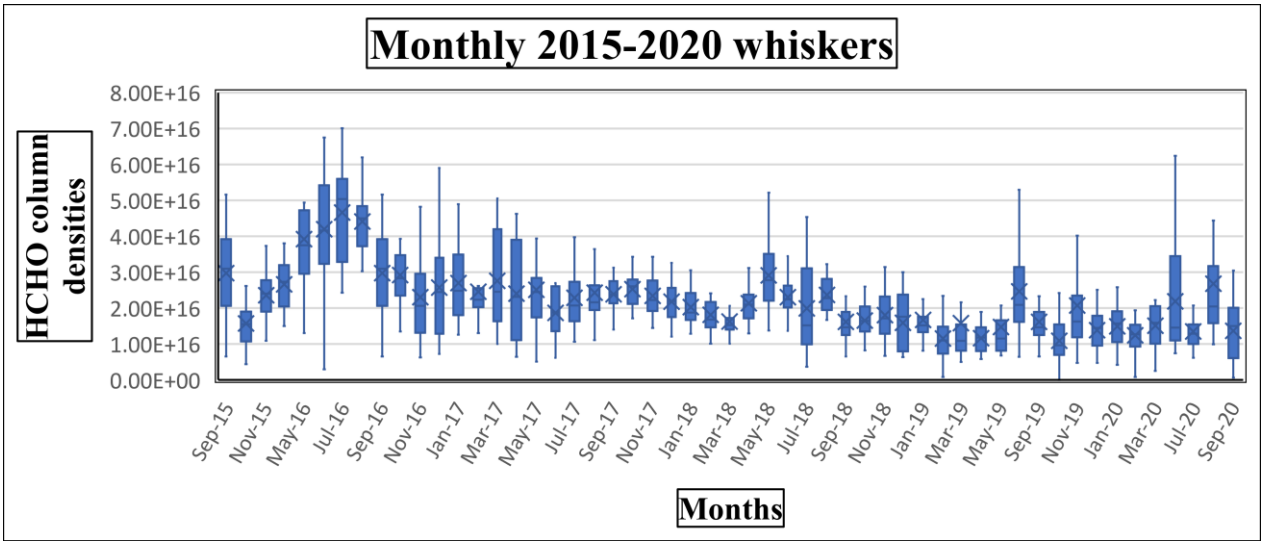

Figure 4. 11: Monthly whiskers of HCHO VCDs over IESE-NUST observed using MAX-DOAS (Sep 2015-Oct 2020).

This is the monthly whisker showing highest HCHO column densities in 2016.

4.6 NDVI Timeseries IESE, NUST

NDVI timeseries at IESE, NUST shows that the HCHO column densities increases from 2015-2020. During these years new plants have been grown at IESE and NUST. For this point data has been extracted using MODIS, data for every 16 days was available.

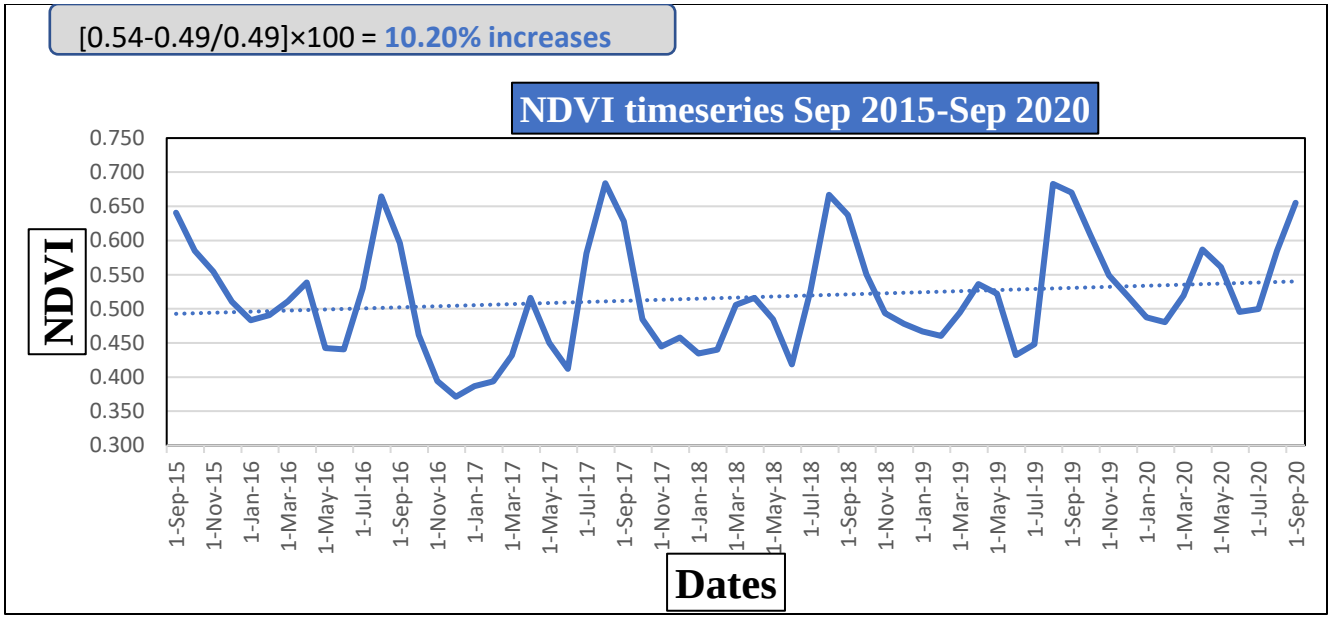

Figure 4. 12: NDVI Timeseries over IESE NUST (MODIS)

4.7 NDVI Timeseries Islamabad

NDVI timeseries at Islamabad shows that the HCHO column densities decreases from Sep 2015-Sep 2020. During these years the plantation has been decreased due to increase in population. For this polygon data has been extracted using MODIS, data for every 16 days was available.

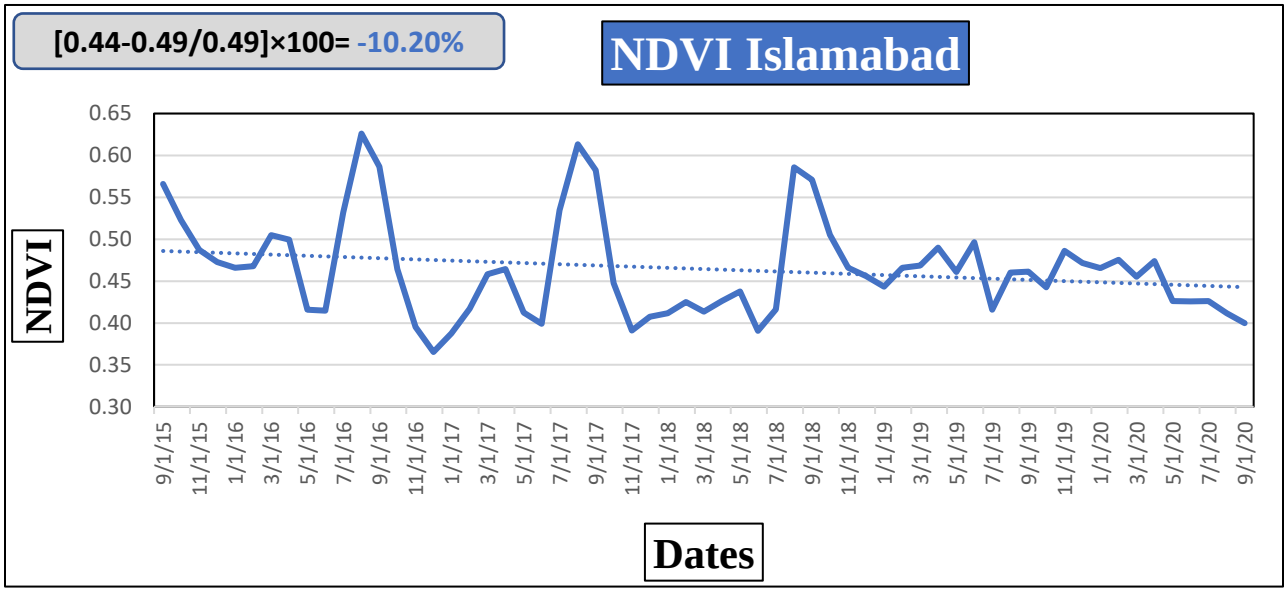

Figure 4. 13: NDVI Timeseries over Islamabad NUST (MODIS)

4.8 CNG consumption

CNG consumption for Sep 2015-Sep 2020 has been calculated. Data was taken from SNGPL, I-9 Islamabad. It shows a significant decrease in trend during study period.

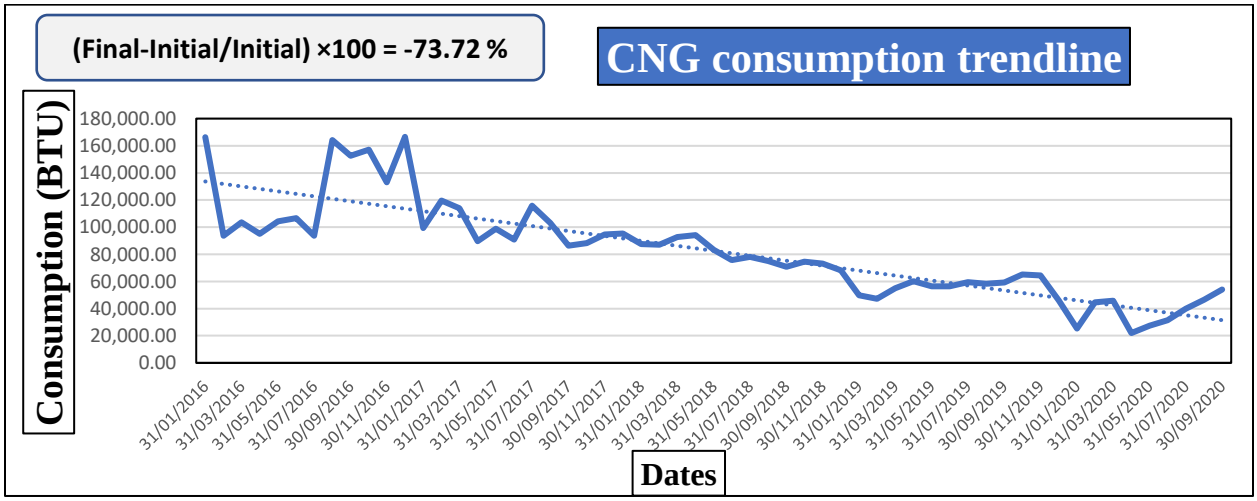

Figure 4. 14: Monthly CNG consumption in Islamabad from 2016 to 2020 (Source SNGPL)

4.9 Temperature Timeseries Sep 2015-Sep 2020

Temperature timeseries from Sep 2015 to Sep 2020 has been shown. It shows that the temperature has been decreased up to 15.92 percent during this period.

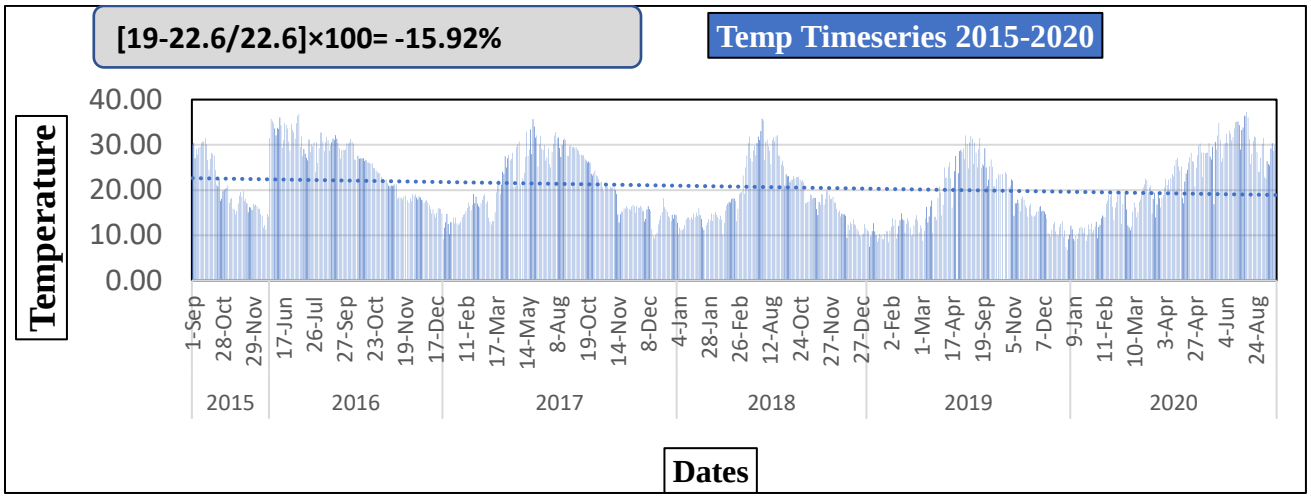

Figure 4. 15: Timeseries of Temperature data at NUST Islamabad from 2015 to 2020 (Source Weather station USPCASE)

4.10 HCHO Mixing Ratio

A mixing ratio of HCHO was calculated by converting HCHO VCDs derived from MAX-DOAS ground-based monitoring to HCHO mixing ratio in part per billion by volume (PPBV) considering that HCHO is concentrated near the ground in the ambient air, close to its source of emission. We have selected a suitable altitude of 500m. The result shows that the average daily HCHO concentration monitored during the study period was observed to be mostly within WHO limits.

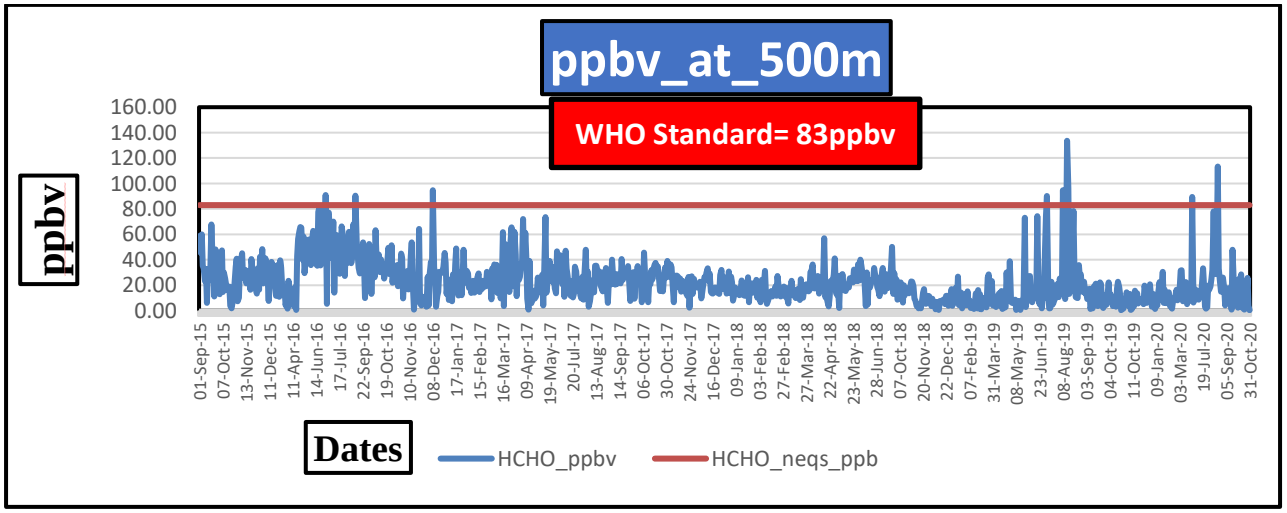

Figure 4. 16: Table showing HCHO mixing ratio.

4.11 Satellite validation of MAX-DOAS data

4.11.1 IESE-NUST site

The continuously monitored HCHO data at IESE-NUST by using MAX-DOAS was validated by comparing it with TropOMI and OMI data. The monthly average Tropospheric HCHO data from TropOMI was only available from October 2018 to date. While the data for the previous years i-e September 2015 to September 2018 was taken from OMI. The tropospheric column daily averages from TropOMI and OMI was compared with MAX-DOAS data. The satellite data underestimated the ground-based HCHO MAX-DOAS observations. A correlation with Pearson values of **0.61** and **0.63** was observed for comparison of both Tropospheric Ozone Monitoring Instrument (TropOMI) i-e Oct 2018-Oct 2020 and Ozone Monitoring Instrument (OMI) Sep 2015-Sep 2018 with ground-based results respectively.

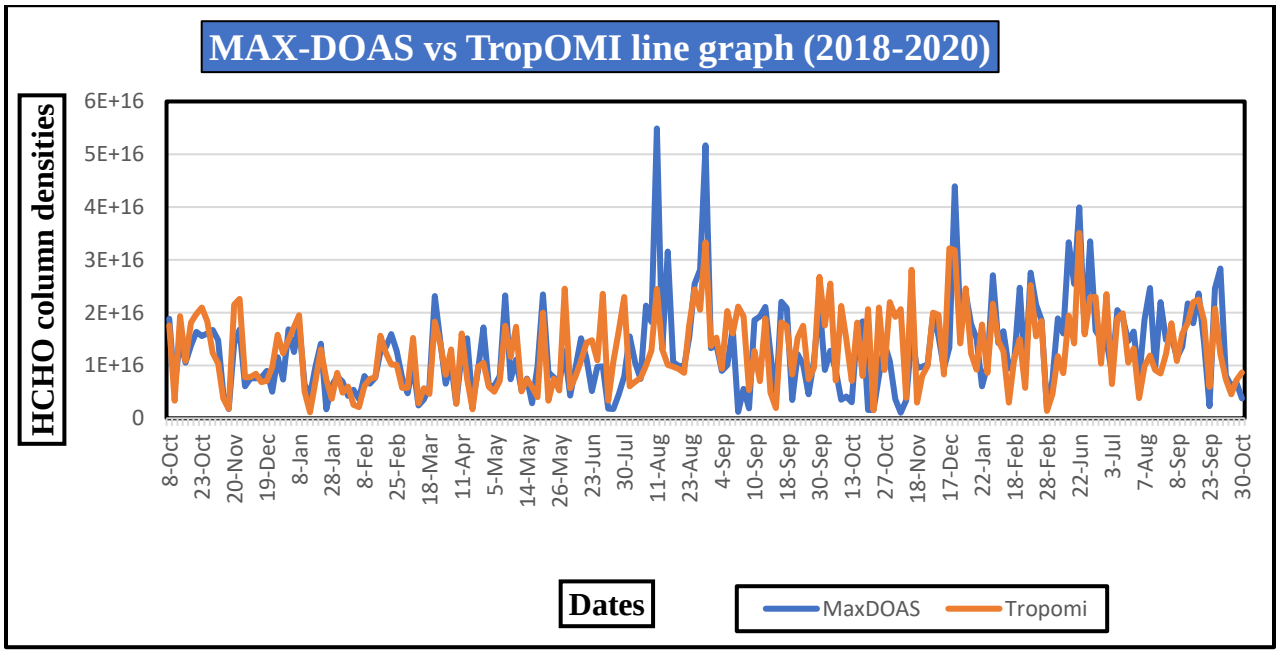

Figure 4. 17: **Line graph showing validation of TropOMI with MAX-DOAS (Oct 2018-Oct 2020)**

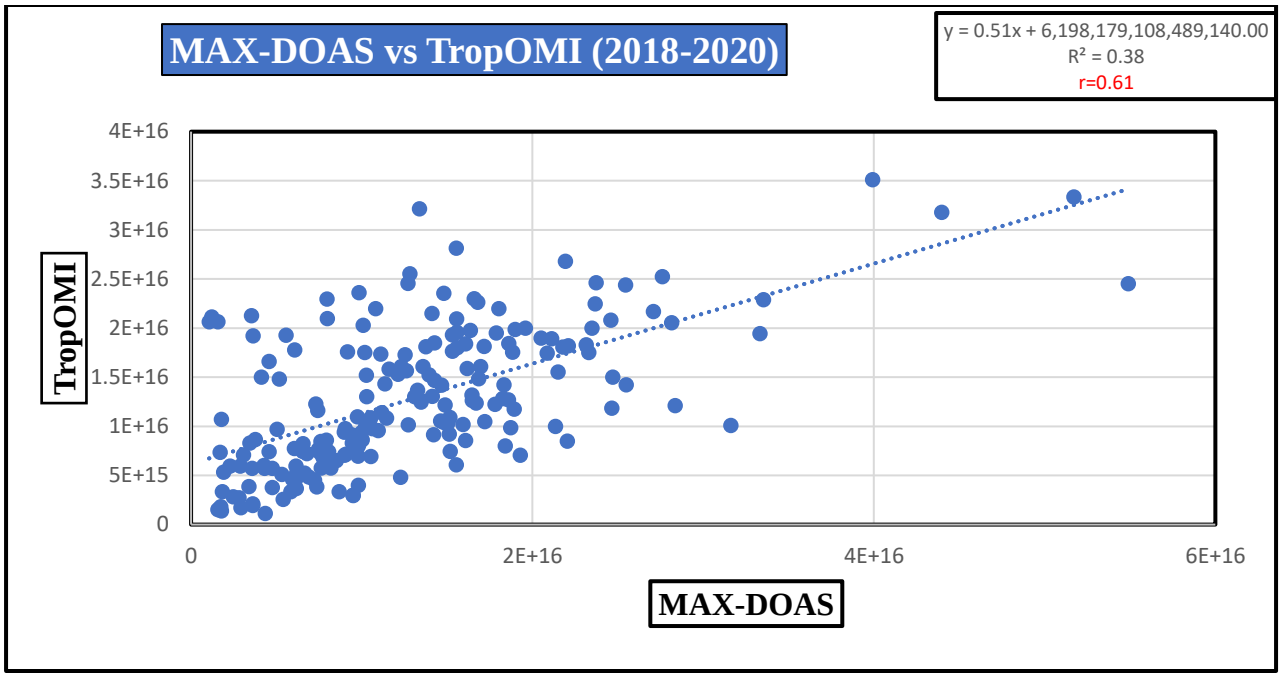

Figure 4. 18: MAX-DOAS Correlation with TROPOMI (2018-2020)

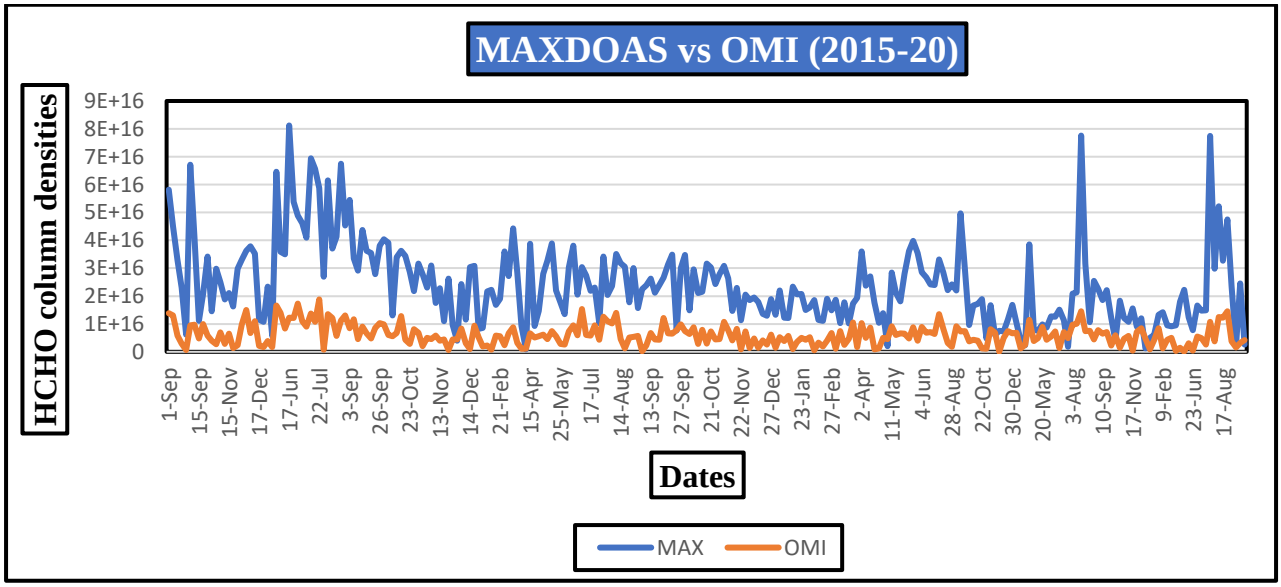

Figure 4. 19: Line graph showing validation of OMI with MAX-DOAS (Sep 2015-Sep 2020)

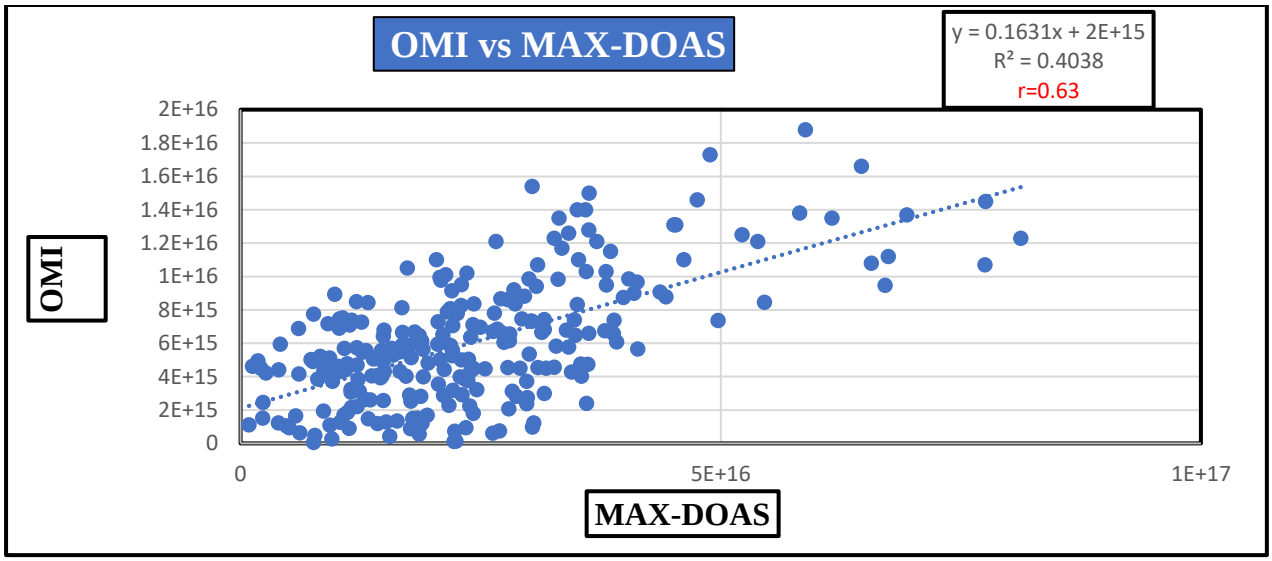

Figure 4. 20*:* MAX-DOAS Correlation with OMI (Sep 2015-Sep 2020)

4.11.2 Temperature dependence of HCHO Concentrations

Plants release NMVOCs under heat stress, which are the precursors of HCHO in the atmosphere and contribute majorly to HCHO formation in the atmosphere. To validate this point temperature data were compared with ground-based MAX-DOAS VCDs observed during the study period. For Oct 2018 to Oct 2020 temperature showed a correlation of **0.56** with MAX-DOAS measurements over Islamabad.

From September 2015-October 2020 temperature shows a correlation of **0.64** with Formaldehyde VCDs.

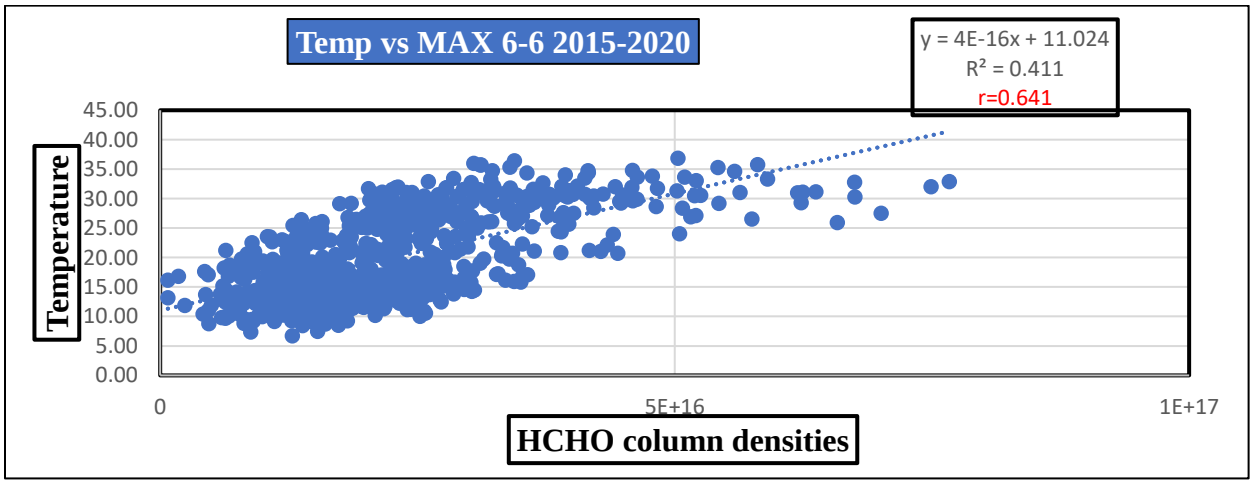

Figure 4. 21: Comparison of MAX-DOAS VCDs vs Temperature over Islamabad (2015-2020)

4.11.3 GHI dependence of HCHO concentration

GHI stands for Global horizontal irradiance. It is the total radiation receives by a surface horizontal to the ground. The result shows that GHI varies inversely with Formaldehyde VCDs. Solar radiations break down Formaldehyde when it strikes on it, so more GHI will result in the breakdown of more formaldehyde VCDs. This study shows a negative correlation of 0.069.

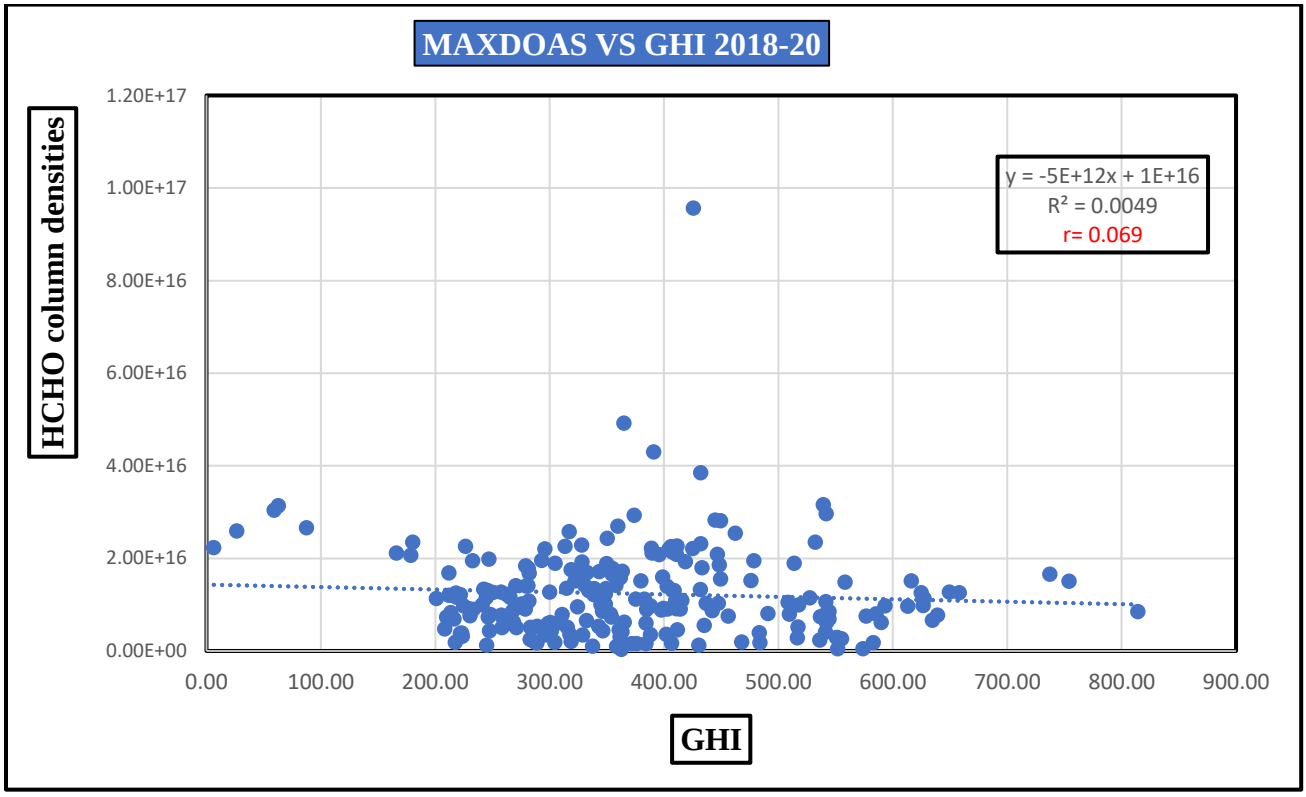

Figure 4. 22: Comparison of MAX-DOAS VCDs vs GHI over Islamabad (Oct 2018-Oct 2020)

From 2015-2020 the GHI shows a similar trend with Average VCDs as above. It Shows a negative correlation of 0.09.

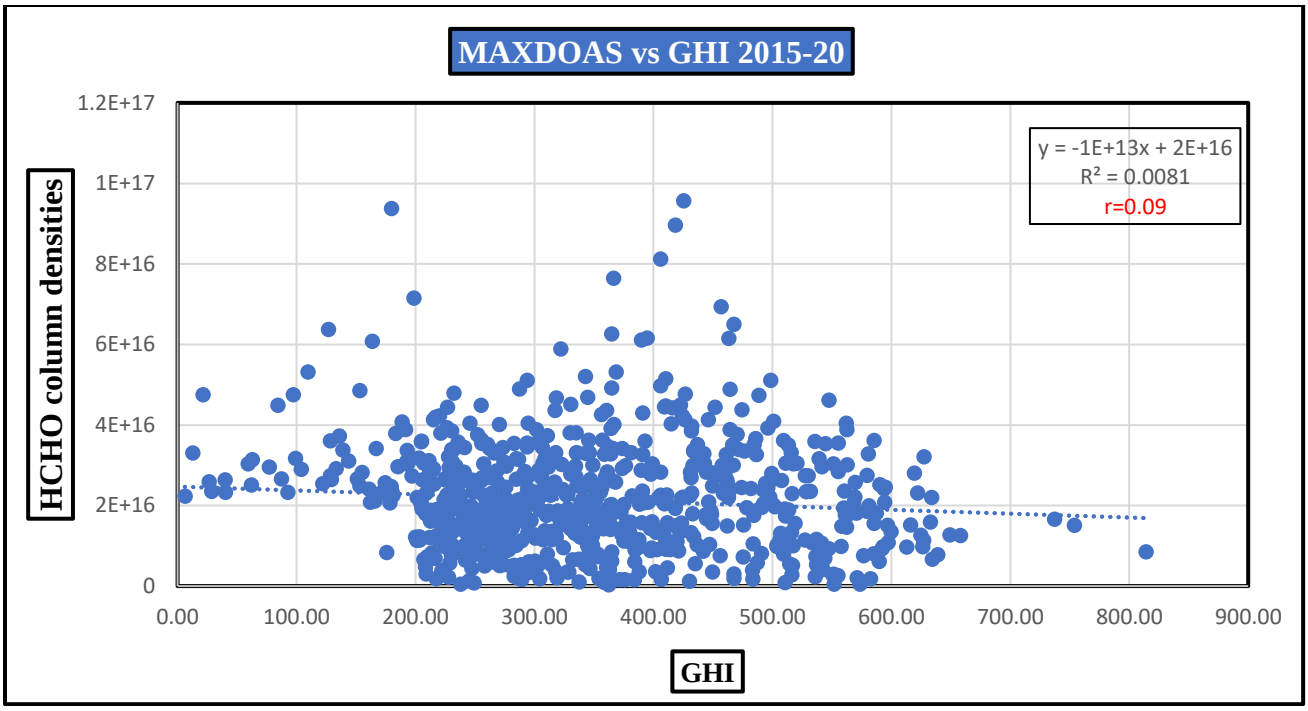

Figure 4. 23: Comparison of MAX-DOAS monthly average VCDs vs monthly average GHI over Islamabad (Sep 2015-Sep 2020)

4.11.4 CNG dependance on HCHO concentration

The result shows that the CNG consumption varies directly with HCHO column densities. It shows 0.64 correlation with HCHO column densities.

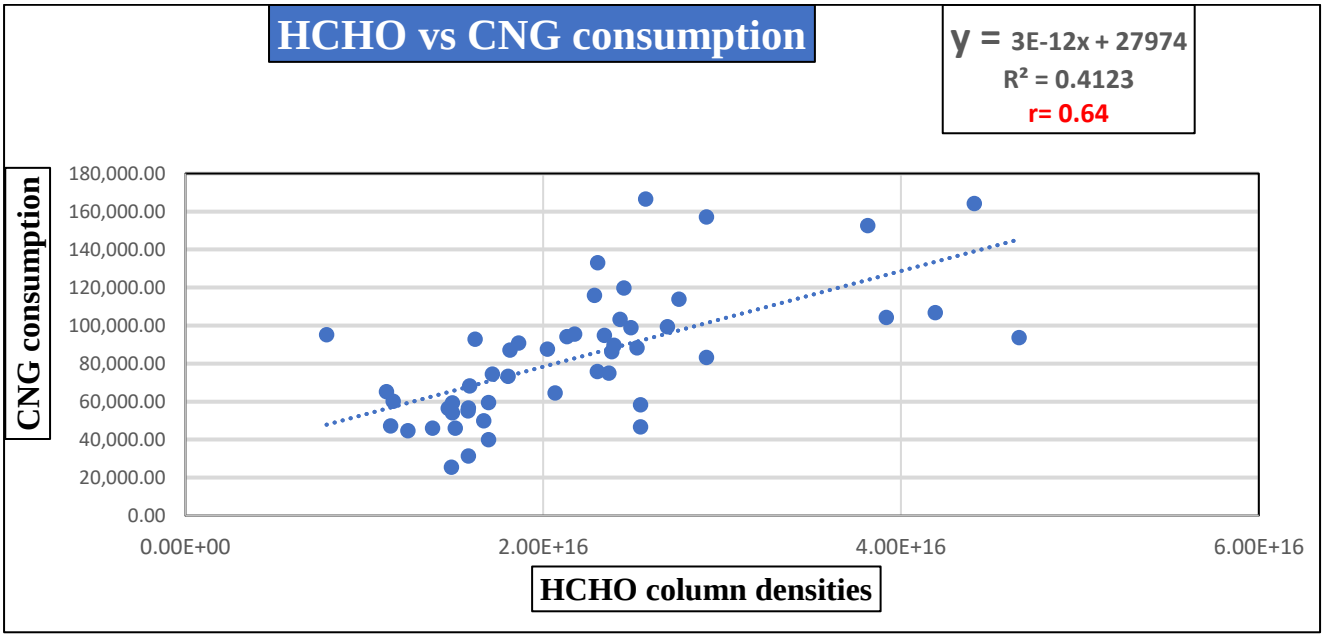

Figure 4.24: Comparison of MAX-DOAS monthly average VCDs vs CNG consumption for Islamabad (Sep 2015-Sep 2020)

4.12 Impact of COVID-19 Lockdown

During the lockdown, the market was closed so is the transport. Only a few shops were allowed to open with SOPs. To analyze the impact of lockdown on HCHO VCDs, the data was taken in two intervals from 1st March 2019 to 22nd March 2019, and 23rd March 2019 to 15th April 2019, this data was then compared with 2020. 1ST March 2020 to 22nd March 2020 was taken as Pre-Lockdown period and 23rd March 2020 to 15th April 2020 was considered as lockdown period. It was observed that HCHO VCDs decrease up to 9**%** during the lockdown period. As a whole Formaldehyde VCDs decreases with the lockdown. This is shown in the table below.

Dates	HCHO column densities	Percentage difference
1 March 2019-22 March 2019	1.06E+16	-22.06%
23 March 2019-15 Apr 2019	1.36E+16	Benchmark
1march 2020-22 March 2020	1.05E+16	-22.80%
23 March 2020-15 Apr 2020	1.23E+16	-9.66%

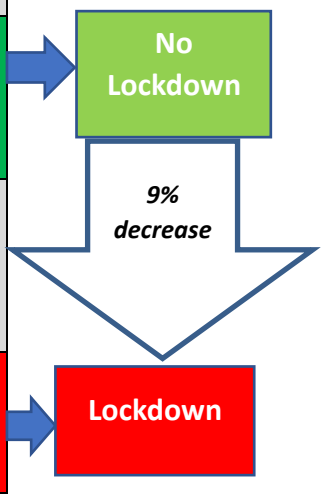

Figure 4. 25: Table showing Impact of Smart lockdown on HCHO VCDs

Chapter 5

Conclusions and Recommendations

5.1 Conclusions

HCHO mixing ratios measured during the study period of September 2015- October 2020 over IESE-NUST, Islamabad was found to be higher in summer than the WHO threshold value of 83 PPBV. The HCHO diurnal cycle calculated for different seasons revealed that maximum concentrations were found during summer and minimum in winter mainly due to the lower temperature, OH production, lesser photolysis, and lower biogenic emissions of VOCs in winter. The VCDs of HCHO were compared with temperature data over Islamabad and a positive correlation of **0.64** was found. While the GHI values over IESE show a negative correlation of **0.09** with the HCHO VCDs measured at IESE. Satellite data over IESE with the ground data showed a correlation of 0.61 and 0.63 with TropOMI and OMI respectively. The satellite observations were observed to be underestimating the ground-based values. A comparison of data from 2020 with 2019 shows that lockdown has a significant effect on Formaldehyde concentration. This indicates that by decreasing mass transit we can control air quality deterioration.

5.2 Recommendations

Based on our findings, the following are some of the recommendations for improving the air quality of Pakistan and promoting continuous air quality monitoring practices:

1. NEQS (National Environmental Quality Standards) should be formulated for HCHO concentrations in the ambient air.
2. Field Campaigns in forest areas of Pakistan should be conducted in each season of the year to generate a database of air pollutants in these areas and also to investigate the seasonal trend.
3. Continuous air quality monitoring stations should be developed throughout the

country for air quality assessment and effective pollution control techniques should be adopted for air pollution abatement.

4. Media campaigns should be run effectively for generating concern among the general public for the air quality of the country.

5. The public should be given open access to air quality and health data by both government and non-government agencies.

6. Awareness among the school children, citizen groups, etc. about air pollution, its consequences, and control should be spread for generating a sense of responsibility among them.

7. The use of a mass transit system and the adoption of other sustainable ways of transportation such as carpooling should be promoted in the mega-cities of the country.

8. Improved understanding of the production of HCHO precursors such as isoprene from vegetation is required through extensive and continuous monitoring.

References

Anand, S. S., Philip, B. K., & Mehendale, H. M. (2014). Volatile Organic Compounds. In *Encyclopedia of Toxicology: Third Edition* (Third Edit, Vol. 4). Elsevier. https://doi.org/10.1016/B978-0-12-386454-3.00358-4

Anjum, M. S., Ali, S. M., Imad-ud-din, M., Subhani, M. A., Anwar, M. N., Nizami, A. S., Ashraf, U., & Khokhar, M. F. (2021). An Emerged Challenge of Air Pollution and Ever-Increasing Particulate Matter in Pakistan; A Critical Review. *Journal of Hazardous Materials*, *402*(September 2020), 123943. https://doi.org/10.1016/j.jhazmat.2020.123943

Chen, J., Li, C., Ristovski, Z., Milic, A., Gu, Y., Islam, M. S., Wang, S., Hao, J., Zhang, H., He, C., Guo, H., Fu, H., Miljevic, B., Morawska, L., Thai, P., LAM, Y. F., Pereira, G., Ding, A., Huang, X., & Dumka, U. C. (2017). A review of biomass burning: Emissions and impacts on air quality, health, and climate in China. *Science of the Total Environment*, *579*(November 2016), 1000–1034. https://doi.org/10.1016/j.scitotenv.2016.11.025

Chou, C. H. S. J., & Williams-Johnson, M. (1998). Health Effects Classification and Its Role in the Derivation of Minimal Risk Levels: Neurological Effects. *Toxicology and Industrial Health*, *14*(3), 455–471. https://doi.org/10.1177/074823379801400305

Dickinson, R. E., & Cicerone, R. J. (1986). Future global warming from atmospheric trace gases. *Nature*, *319*(6049), 109–115. https://doi.org/10.1038/319109a0

Fini, J. B., Mughal, B. B., Le Mével, S., Leemans, M., Lettmann, M., Spirhanzlova, P., Affaticati, P., Jenett, A., & Demeneix, B. A. (2017). Human amniotic fluid contaminants alter thyroid hormone signalling and early brain development in Xenopus embryos. *Scientific Reports*, *7*(October 2016), 1–12. https://doi.org/10.1038/srep43786

Gratsea, M., Vrekoussis, M., Richter, A., Wittrock, F., Schönhardt, A., Burrows, J., Kazadzis, S., Mihalopoulos, N., & Gerasopoulos, E. (2016). Slant column MAX-DOAS measurements of nitrogen dioxide, formaldehyde, glyoxal and oxygen dimer in the urban environment of Athens. *Atmospheric Environment*, *135*, 118–131. https://doi.org/10.1016/j.atmosenv.2016.03.048

Guenther, A., Geron, C., Pierce, T., Lamb, B., Harley, P., & Fall, R. (2000). Natural emissions of non-methane volatile organic compounds, carbon monoxide, and oxides of nitrogen from North

America. *Atmospheric Environment*, *34*(12–14), 2205–2230. https://doi.org/10.1016/S1352-2310(99)00465-3

Hönninger, G., von Friedeburg, C., & Platt, U. (2004). Multi axis differential optical absorption spectroscopy (MAX-DOAS). *Atmospheric Chemistry and Physics*, *4*(1), 231–254. https://doi.org/10.5194/acp-4-231-2004

IARC Working Group on the Evaluation of Carcinogenic Risks to Humans. (2012). Chemical agents and related occupations. *IARC Monographs on the Evaluation of Carcinogenic Risks to Humans / World Health Organization, International Agency for Research on Cancer*, *100*(Pt F), 9–562.

Javed, Z., Wang, Y., Xie, M., Tanvir, A., Rehman, A., Ji, X., Xing, C., Shakoor, A., & Liu, C. (2020). Investigating the impacts of the COVID-19 lockdown on trace gases using ground-based MAX-DOAS observations in Nanjing, China. *Remote Sensing*, *12*(23), 1–17. https://doi.org/10.3390/rs12233939

Khan, W. A., Khokhar, M. F., Shoaib, A., & Nawaz, R. (2018). Monitoring and analysis of formaldehyde columns over Rawalpindi-Islamabad, Pakistan using MAX-DOAS and satellite observation. *Atmospheric Pollution Research*, *9*(5), 840–848. https://doi.org/10.1016/j.apr.2017.12.008

Khokhar, M. F., Khalid, T., Yasmin, N., & De Smedt, I. (2015). Spatio-temporal analyses of formaldehyde over Pakistan by using SCIAMACHY and GOME-2 observations. *Aerosol and Air Quality Research*, *15*(5), 1760–1773. https://doi.org/10.4209/aaqr.2014.12.0339

Khokhar, M. F., Naveed, S. I., Butt, J. K., & Abbas, Z. (2016). Comparative analysis of atmospheric glyoxal column densities retrieved from MAX-DOAS observations in Pakistan and during MAD-CAT field campaign in Mainz, Germany. *Atmosphere*, *7*(5). https://doi.org/10.3390/atmos7050068

Kim, K. H., Jahan, S. A., & Lee, J. T. (2011). Exposure to formaldehyde and its potential human health Hazards. *Journal of Environmental Science and Health - Part C Environmental Carcinogenesis and Ecotoxicology Reviews*, *29*(4), 277–299. https://doi.org/10.1080/10590501.2011.629972

Li, X., Brauers, T., Hofzumahaus, A., Lu, K., Li, Y. P., Shao, M., Wagner, T., & Wahner, A. (2013). MAX-DOAS measurements of NO2, HCHO and CHOCHO at a rural site in Southern China. *Atmospheric Chemistry and Physics*, *13*(4), 2133–2151. https://doi.org/10.5194/acp-13-2133-2013

Luecken, D. J., Hutzell, W. T., Strum, M. L., & Pouliot, G. A. (2012). Regional sources of atmospheric formaldehyde and acetaldehyde, and implications for atmospheric modeling. *Atmospheric Environment*, *47*(2), 477–490. https://doi.org/10.1016/j.atmosenv.2011.10.005

Nourian, A., Abba, M. K., & G. Nasr, G. (2021). Measurements and analysis of non-methane VOC (NMVOC) emissions from major domestic aerosol sprays at "source." *Environment International*, *146*. https://doi.org/10.1016/j.envint.2020.106152

Pamler, P. I., Jacob, D. J., Fiore, A. M., Martin, R. V., Chance, K., & Kurosu, T. P. (2003). Mapping isoprene emissions over North America using formaldehyde column observations from space. *Journal of Geophysical Research D: Atmospheres*, *108*(6). https://doi.org/10.1029/2002jd002153

Platt, U., Stutz, J., Stutz, J., Optical, D., Spectroscopy, A., & Environments, S. (2008). Differential Optical Absorption Spectroscopy. *Differential Optical Absorption Spectroscopy*, *174*, 135–136. https://doi.org/10.1007/978-3-540-75776-4

Porter, W. C., Safieddine, S. A., & Heald, C. L. (2017). Impact of aromatics and monoterpenes on simulated tropospheric ozone and total OH reactivity. *Atmospheric Environment*, *169*, 250–257. https://doi.org/10.1016/j.atmosenv.2017.08.048

Ramanathan, V., Crutzen, P. J., Kiehl, J. T., & Rosenfeld, D. (2001). Atmosphere: Aerosols, climate, and the hydrological cycle. *Science*, *294*(5549), 2119–2124. https://doi.org/10.1126/science.1064034

Salthammer, T. (2013). Formaldehyde in the ambient atmosphere: From an indoor pollutant to an outdoor pollutant? *Angewandte Chemie - International Edition*, *52*(12), 3320–3327. https://doi.org/10.1002/anie.201205984

Spracklen, D. V., Carslaw, K. S., Pöschl, U., Rap, A., & Forster, P. M. (2011). Global cloud condensation nuclei influenced by carbonaceous combustion aerosol. *Atmospheric Chemistry and*

Physics, *11*(17), 9067–9087. https://doi.org/10.5194/acp-11-9067-2011

Sprengnether, M., Demerjian, K. L., Donahue, N. M., & Anderson, J. G. (2002). Product analysis of the OH oxidation of isoprene and 1,3-butadiene in the presence of NO. *Journal of Geophysical Research Atmospheres*, *107*(15), ACH 8-1-ACH 8-13. https://doi.org/10.1029/2001JD000716

Tang, J. E., Moore, D. R., Kujbida, G. W., Tarnopolsky, M. A., & Phillips, S. M. (2009). Ingestion of whey hydrolysate, casein, or soy protein isolate: Effects on mixed muscle protein synthesis at rest and following resistance exercise in young men. *Journal of Applied Physiology*, *107*(3), 987–992. https://doi.org/10.1152/japplphysiol.00076.2009

Tanvir, A., Javed, Z., Jian, Z., Zhang, S., Bilal, M., Xue, R., Wang, S., & Bin, Z. (2021). Ground-based max-doas observations of tropospheric no2 and hcho during covid-19 lockdown and spring festival over Shanghai, China. *Remote Sensing*, *13*(3), 1–18. https://doi.org/10.3390/rs13030488

The world health report 1996 - Fighting disease, fostering development. (1997). In *World Health Forum* (Vol. 18, Issue 1, pp. 1–8).

Tian, X., Xie, P., Xu, J., Li, A., Wang, Y., Qin, M., & Hu, Z. (2018). Long-term observations of tropospheric NO2, SO2 and HCHO by MAX-DOAS in Yangtze River Delta area, China. *Journal of Environmental Sciences (China)*, *71*(2), 207–221. https://doi.org/10.1016/j.jes.2018.03.006

United States Protection Agency. (2001). *National Air Quality and Emissions Trends Report , 1999 National Air Quality and Emissions Trends Report ,. March*, 258.

Vrekoussis, T., Kalantaridou, S. N., Mastorakos, G., Zoumakis, E., Makrigiannakis, A., Syrrou, M., Lavasidis, L. G., Relakis, K., & Chrousos, G. P. (2010). The role of stress in female reproduction and pregnancy: An update. *Annals of the New York Academy of Sciences*, *1205*(June 2016), 69–75. https://doi.org/10.1111/j.1749-6632.2010.05686.x

Wang, W., Wu, T., Li, Y., Xie, S., Han, B., Zheng, H., & Ouyang, Z. (2020). Urbanization impacts on natural habitat and ecosystem services in the Guangdong-Hong Kong-Macao "Megacity." *Sustainability (Switzerland)*, *12*(16). https://doi.org/10.3390/su12166675

Watson, J. G., Chow, J. C., & Fujita, E. M. (2001). Review of volatile organic compound source

apportionment by chemical mass balance. *Atmospheric Environment*, *35*(9), 1567–1584. https://doi.org/10.1016/S1352-2310(00)00461-1

WHO. (2014). World Health statistics 2014, World Health Organization. In *World Health Organization*.

Wuebbles, D. J., & Hayhoe, K. (2002). Atmospheric methane and global change. *Earth-Science Reviews*, *57*(3–4), 177–210. https://doi.org/10.1016/S0012-8252(01)00062-9